JPRS-UEQ-91-002
8 FEBRUARY 1991

Foreign Broadcast Information Service 50 ANNIVERSARY 1941 - 1991

# JPRS Report

# Science & Technology

## USSR: Engineering & Equipment

JPRS-UEQ-91-002
8 FEBRUARY 1991

# SCIENCE & TECHNOLOGY

# USSR: ENGINEERING & EQUIPMENT

## CONTENTS

UDC 539.3:534.21

# Magnetoelastic Surface Waves in Half-Space With Surface Electric Current

917F0082A IZVESTIYA AKADEMII NAUK ARMYANSKOY SSR: SERIYA MEKHANIKA in Russian Vol 43 No 1, 1990 (manuscript received 25 Oct 88) pp 3-9

[Article by M. V. Belubekyan, Institute of Mechanics, ArmSSR Academy of Sciences]

[Text] The earliest research on magnetoelastic surface waves in the presence of a constant magnetic field was done by S. Kaliskiy [1]. This work has subsequently been continued by many researchers.

In contrast to other papers, this one considers the case where a magnetic field is set up by electric current flowing over the surface of a half-space. Studies of the propagation of elastic waves in the presence of surface current may have application in nondestructive testing of materials [2].

*1.* Let an elastic half-space occupy region $x_2 \geq 0$ in rectangular coordinate system $(x_1, x_2, x_3)$. Electric current with surface density $J_0$ flows along boundary $x_2 = 0$ in the direction of axis $0x_1$. In the initial (unperturbed) state, the magnetic fields caused by $J_0$ will be constant in regions $x_2 > 0$ and $x_2 < 0$, undergoing a discontinuity (jump) on surface $x_2 = 0$. The magnetic field intensities must be defined to satisfy boundary condition

$$[\overline{H}_0^{(e)} - \overline{H}_0] \times \hat{j} = \frac{4\pi}{c} J_0 \hat{i}$$

Here $\overline{H}_0^{(e)}$, $\overline{H}_0$ are magnetic field intensity vectors where $x_2 < 0$, $x_2 > 0$ respectively, $\hat{i}$, $\hat{j}$, $\hat{k}$ are unit vectors in directions $x_1$, $x_2$ and $x_3$ respectively.

The following three versions are possible for definition of a magnetic field satisfying these conditions:

$$\left.\begin{aligned} &\bar{H}_0 = H_0\hat{k}, \quad \bar{H}_0^{(e)} = -H_0\hat{k} && (1.1)\\ &\bar{H}_0 = 0, \quad \bar{H}_0^{(e)} = -2H_0\hat{k} && (1.2)\\ &\bar{H}_0 = 2H_0\hat{k}, \quad \bar{H}_0^{(e)} = 0 && (1.3) \end{aligned}\right\}_0 = \frac{2\pi}{c} J_0$$

A model for versions (1.2) and (1.3) is a medium in the form of a layer of rather considerable thickness with current flowing over its surfaces with surface density $J_o$. Where currents over the surfaces have the same direction, the magnetic field cannot penetrate into the layer, and we arrive at version (1.2). Version (1.3) is the result in the case where surface currents are oppositely directed.

According to (1.1)-(1.3, the components of the Maxwell tensors for the corresponding versions take the form (only non-zero components are given):

$$T_{110} = T_{110}^{(e)} = -\frac{1}{8\pi} H_0^2, \quad T_{220} = T_{220}^{(e)} = -\frac{1}{8\pi} H_0^2, \quad T_{330} = T_{330}^{(e)} = \frac{1}{8\pi} H_0^2 \tag{1.4}$$

$$T_{110}^{(e)} = -\frac{1}{2\pi} H_0^2, \quad T_{220}^{(e)} = -\frac{1}{2\pi} H_0^2, \quad T_{330}^{(e)} = \frac{1}{2\pi} H_0^2 \tag{1.5}$$

$$T_{110} = -\frac{1}{2\pi} H_0^2, \quad T_{220} = -\frac{1}{2\pi} H_0^2, \quad T_{330} = \frac{1}{2\pi} H_0^2 \tag{1.6}$$

Here and below, the permeabilities of the material of the half-space $x_2 \geq 9$ and of the medium outside of the half-space are assumed to be equal to unity.

In the first version (1.4), the components of the Maxwell tensor are continuous on boundary $x_2 = 0$, and therefore the initial stressed state is zero ($\sigma_{ij}^o = 0$). In the second (1.5) and third (1.6) versions, component $T_{330}$ undergoes a discontinuity on boundary $x_2 = 0$, giving rise to initial stresses.

To determine the initial stressed state, it is necessary to satisfy boundary conditions ($x_2 = 0$)

$$\sigma_{2j}^0 + T_{2j0} = T_{2j0}^{(e)} \tag{1.7}$$

The stressed state also depends on conditions as $x_1 \to \pm\infty$, $x_2 \to \pm\infty$. The simplest stressed state results when conditions

$$\lim_{x_1 \to \pm\infty} \sigma_{11}^0 = 0, \quad \lim_{x_3 \to \pm\infty} \sigma_{33}^0 = 0 \tag{1.8}$$

are satisfied.

In this context, all components of the stress tensor are equal to zero except $\sigma_{22}^o$, which is defined as follows

$$\sigma_{22}^0 = -\frac{1}{2\pi} H_0^2 \quad \text{and} \quad \sigma_{22}^0 = \frac{1}{2\pi} H_0^2 \tag{1.9}$$

(for the second and third versions respectively).

Formulation of the problem of wave propagation in the given three versions of the initial state will depend on the physical properties of the material of the half-space. Here problems are possible where the material is either a dielectric, or an ideal conductor, or a superconductor.

2. Of considerable significance in derivation of boundary conditions is allowance for the behavior of the normal to the perturbed surface of the half-space [3].

Let the perturbed surface of the half-space be defined by the equation

$$x_2 = u_2(x_1, 0, x_3, t) \tag{2.1}$$

Then the approximate (linearized) expression for the normal to the perturbed surface takes the form

$$\hat{n} \simeq \frac{\partial u_2}{\partial x_1} \hat{i} - \hat{j} + \frac{\partial u_2}{\partial x_3} \hat{k} \tag{2.2}$$

To derive linearized boundary conditions on surface $x_2 = 0$, we will start from the following general conditions; when $x_2 = 0$

$$[\bar{H}^{(e)} - \bar{H}] \cdot \hat{n} = 0, \quad [\bar{E}^{(e)} - \bar{E}] \times \hat{n} = \frac{1}{c} \frac{\partial u_2}{\partial t} [\bar{H}^{(e)} - \bar{H}]$$

$$(\bar{\sigma}_i + \bar{T}_i) \cdot \hat{n} = \bar{T}_i^{(e)} \cdot \hat{n} \tag{2.3}$$

where

$$\bar{\sigma}_i = \sigma_{i1}\hat{i} + \sigma_{i2}\hat{j} + \sigma_{i3}\hat{k}, \quad \bar{T}_i = T_{i1}\hat{i} + T_{i2}\hat{j} + T_{i3}\hat{k} \tag{2.4}$$

Using expressions

$$\sigma_{ij} = \sigma_{ij}^0 + \sigma_{ij}', \quad \bar{H} = \bar{H}_0 + \bar{h}, \quad \bar{E} = \bar{e} \tag{2.5}$$

for the perturbed state, and linearizing condition (2.3) with allowance for smallness of perturbations and with consideration of (1.1-1.6), (1.9), (2.2), we get the boundary conditions on the surface of the half-space.

In all three versions,. boundary conditions for components of the perturbed electromagnetic field are the same, and take the form

$$h_2 - h_2^{(e)} = 2H_0 \frac{\partial u_2}{\partial x_3}, \quad e_1 - e_1^{(e)} = -\frac{2H_0}{c} \frac{\partial u_2}{\partial t}, \quad e_3 = e_3^{(e)} \quad (x_2 = 0) \tag{2.6}$$

Conditions for stresses for versions (1.1)-(1.3) in the corresponding sequence are obtained in the form

$$\sigma_{12}=0, \quad \sigma_{22}-\frac{H_0}{4\pi}h_3=\frac{H_0}{4\pi}h_3^{(e)}, \quad \sigma_{32}+\frac{H_0}{4\pi}h_2=-\frac{H_0}{4\pi}h_2^{(e)} \tag{2.7}$$

$$\sigma_{12}=\frac{H_0^2}{2\pi}\frac{\partial u_2}{\partial x_1}, \quad \sigma_{22}=\frac{H_0}{2\pi}h_3^{(e)}, \quad \sigma_{32}+\frac{H_0^2}{2\pi}\frac{\partial u_2}{\partial x_3}=-\frac{H_0}{2\pi}h_2^{(e)} \tag{2.8}$$

$$\sigma_{12}=-\frac{H_0^2}{2\pi}\frac{\partial u_2}{\partial x_1}, \quad \sigma_{22}-\frac{H_0}{2\pi}h_3=0, \quad \sigma_{32}+\frac{H_0}{2\pi}h_2=\frac{H_0^2}{2\pi}\frac{\partial u_2}{\partial x_3} \tag{2.9}$$

In (2.7)-(2.9) and below, the primes of $\sigma'_{ij}$ have been omitted.

Let us take a look at some special problems of surface wave propagation.

*3.* Let the initial magnetic field correspond to version (1.1). The material of half-space $x_2 > 0$ is a dielectric. The problems of planar and antiplanar deformation relative to planes $(x_1, x_2)$ and $(x_2, x_3)$ are separated.

Let us consider the plane problem where displacements and components of the perturbed electromagnetic field do not depend on coordinate $x_2$.

We give the equations and boundary conditions of the problem. The equations of the theory of elasticity in displacements

$$c_1^2\frac{\partial^2 u_1}{\partial x_1^2}+c_2^2\frac{\partial^2 u_1}{\partial x_2^2}+(c_1^2-c_2^2)\frac{\partial^2 u_2}{\partial x_1\partial x_2}=\frac{\partial^2 u_1}{\partial t^2}$$

$$x_2>0 \tag{3.1}$$

$$c_2^2\frac{\partial^2 u_2}{\partial x_1^2}+c_1^2\frac{\partial^2 u_2}{\partial x_2^2}+(c_1^2-c_2^2)\frac{\partial^2 u_1}{\partial x_1\partial x_2}=\frac{\partial^2 u_2}{\partial t^2}$$

Equations of electrodynamics in region $x_2 > 0$

$$\frac{\partial h_3}{\partial x_2}=\frac{\varepsilon}{c}\frac{\partial e_1}{\partial t}, \quad -\frac{\partial h_3}{\partial x_1}=\frac{\varepsilon}{c}\frac{\partial e_2}{\partial t}, \quad \frac{\partial e_2}{\partial x_1}-\frac{\partial e_1}{\partial x_2}=-\frac{1}{c}\frac{\partial h_3}{\partial t}, \quad \frac{\partial e_1}{\partial x_1}+\frac{\partial e_2}{\partial x_2}=0 \tag{3.2}$$

in region $x_2 < 0$

$$\frac{\partial h_3^{(e)}}{\partial x_2}=\frac{1}{c}\frac{\partial e_1^{(e)}}{\partial t}, \quad -\frac{\partial h_3^{(e)}}{\partial x_1}=\frac{1}{c}\frac{\partial e_2^{(e)}}{\partial t}, \quad \frac{\partial e_2^{(e)}}{\partial x_1}-\frac{\partial e_1^{(e)}}{\partial x_2}=-\frac{1}{c}\frac{\partial h_3^{(e)}}{\partial t}$$

$$\frac{\partial e_1^{(e)}}{\partial x_1}+\frac{\partial e_2^{(e)}}{\partial x_2}=0 \tag{3.3}$$

According to (2.6) and (2.7), the required boundary conditions at $x_2 = 0$ take the form

$$e_1 - e_1^{(e)} = -\frac{2H_0}{c}\frac{\partial u_2}{\partial t}, \quad \frac{\partial u_1}{\partial x_2} + \frac{\partial u_2}{\partial x_1} = 0$$

$$(\lambda + 2G)\frac{\partial u_2}{\partial x_2} + \lambda\frac{\partial u_1}{\partial x_1} - \frac{H_0}{4\pi}h_3 = \frac{H_0}{4\pi}h_3^{(e)} \tag{3.4}$$

Representing the sought functions in the form

$$f(x_1, x_2, t) = f_0(x_2)\exp i(\omega t - kx_1)$$

and following the scheme of solution of the problem of Rayleigh surface waves [4], we get an equation that determines the velocity of a surface wave (it is assumed that $\varepsilon = 1$, $\omega^2/c^2 \ll 1$)

$$(2-\eta+\varkappa_1\sqrt{1-\theta\eta}\,\eta)(2-\eta) - 4\sqrt{1-\eta}\sqrt{1-\theta\eta} \tag{3.5}$$

where

$$\eta = \frac{\omega^2}{k^2c_2^2}, \quad \theta = \frac{c_1^2}{c_2^2}, \quad \varkappa_1 = \frac{H_0^2}{2\pi\rho c^2}$$

For $x_1 = 0$, equation (3.5) coincides with the Rayleigh equation. Just as for the Rayleigh equation, it is shown that equation (3.5) has only one real root satisfying condition $0 < \eta < 1$.

Let us give the equations of the corresponding antiplanar problem.

The equation of the theory of elasticity in region $x_2 > 0$ takes the form

$$c_1^2\left(\frac{\partial^2 u_3}{\partial x_1^2} + \frac{\partial^2 u_3}{\partial x_2^2}\right) = \frac{\partial^2 u_3}{\partial t^2} \tag{3.6}$$

The equations of electrodynamics in region $x_2 > 0$

$$\frac{\partial h_2}{\partial x_1} = \frac{\partial h_1}{\partial x_2} = \frac{\varepsilon}{c}\frac{\partial e_3}{\partial t}, \quad \frac{\partial e_3}{\partial x_2} = -\frac{1}{c}\frac{\partial h_1}{\partial t}, \quad \frac{\partial e_3}{\partial x_1} = \frac{1}{c}\frac{\partial h_2}{\partial t}, \quad \frac{\partial h_1}{\partial x_1} + \frac{\partial h_2}{\partial x_2} = 0 \tag{3.7}$$

in region $x_2 < 0$

$$\frac{\partial h_2^{(e)}}{\partial x_1} - \frac{\partial h_1^{(e)}}{\partial x_2} = \frac{1}{c}\frac{\partial e_3^{(e)}}{\partial t}, \quad \frac{\partial e_3^{(e)}}{\partial x_2} = -\frac{1}{c}\frac{\partial h_1^{(e)}}{\partial t}, \quad \frac{\partial e_3^{(e)}}{\partial x_1} = \frac{1}{c}\frac{\partial h_2^{(e)}}{\partial t}, \quad \frac{\partial h_1^{(e)}}{\partial x_1} + \frac{\partial h_2^{(e)}}{\partial x_2} = 0 \tag{3.8}$$

Boundary conditions at $x_2 = 0$ take the form

$$h_3 = h_2^{(e)}, \quad e_3 = e_3^{(e)}, \quad G\frac{\partial u_3}{\partial x_2} + \frac{H_0}{2\pi}h_3 = 0 \tag{3.9}$$

We have the task of finding the solutions of equations (3.6)-(3.8) that satisfy boundary conditions (3.9) and conditions of damping as $x_2 \to \pm\infty$.

In solving the problem in this formulation, we come to the necessity of an additional boundary condition at $x_2 = 0$. This condition is given in the form

$$h_1^{(e)} - h_1 = \frac{4\pi}{c} J_0 \frac{\partial u_3}{\partial x_1} \tag{3.10}$$

which is due to the jump in the tangential component of the magnetic field in consequence of a change in the direction of the surface current.

With allowance for additional condition (3.10), the problem is completely defined. Solution of the problem shows that there is a purely shear surface wave with velocity defined by the formula

$$\eta_1 = 1 - \left(\frac{H_0^2}{2\pi G}\right)^2 \tag{3.11}$$

*4.* Let the initial magnetic field be assigned in form (1.3) (third version). It is assumed that the ideal conductor model is applicable to the material of medium $x_2 > 0$. It is further assumed that the sought values do not depend on coordinate $x_3$. In this case, the problem of plane deformation leads to solution of the following equations ($V_2^2 = H_0^2/\pi\rho$):

$$\begin{gathered}(c_1^2 + V_1^2)\frac{\partial^2 u_1}{\partial x_1^2} + \left(c_2^2 + \frac{V_1^2}{2}\right)\frac{\partial^2 u_1}{\partial x_2^2} + (c_1^2 - c_2^2 + V_1^2)\frac{\partial^2 u_2}{\partial x_1 \partial x_2} = \frac{\partial^2 u_1}{\partial t^2} \\ c_2^2 \frac{\partial^2 u_2}{\partial x_1^2} + \left(c_1^2 + \frac{3V_1^2}{2}\right)\frac{\partial^2 u_2}{\partial x_2^2} + (c_1^2 - c_2^2 + V_1^2)\frac{\partial^2 u_1}{\partial x_1 \partial x_2} = \frac{\partial^2 u_2}{\partial t^2}\end{gathered} \tag{4.1}$$

for conditions on boundary $x_2 = 0$

$$\left(\lambda - \frac{H_0^2}{\pi}\right)\frac{\partial u_1}{\partial x_1} + \left(\lambda - \frac{H_0^2}{\pi} + 2G\right)\frac{\partial u_2}{\partial x_2} = 0, \quad G\frac{\partial u_1}{\partial x_2} + \left(G + \frac{H_0^2}{2\pi}\right)\frac{\partial u_2}{\partial x_1} = 0 \tag{4.2}$$

The solution of equation (4.1) with condition (4.2) and the condition of damping at infinity ($x_2 \to \infty$) shows that the condition of existence of a surface wave is the same as in the Rayleigh problem ($0 < \eta < 1$). The equation that defines the velocity of the surface wave takes the form

$$\begin{gathered}(2 + \beta/2 - \eta_1)\{(1 + 6\beta)[2 + \beta(-1/2 + 4\beta + 9\beta/2)] - (1 - 9\beta)\eta_1\} = \\ = 4(1 + 6\beta)^{3/2}(1 + 3\beta/2)^{1/2}(1 + \beta/2)^{1/2}(1 - \beta/4)(1 - \eta_1)^{1/2}(1 - 9\eta_1)^{1/2}, \quad \beta = V_1^2/c_2^2\end{gathered} \tag{4.3}$$

Investigation of equation (4.3) relative to the velocity of the surface wave $\eta$ shows that the equation has two real roots in interval (0, 1). One root corresponds to the velocity of the ordinary Rayleigh wave with allowance for the influence of the magnetic field. The other root shows the presence of a surface wave with a velocity much lower than that of the Rayleigh wave. This velocity can be computed from the following approximate formula:

$$\eta \approx \frac{3H_0^2}{2\pi(\lambda+G)}$$

The problem outlined in this section has also been considered in [5-7].

REFERENCES


1. Kapelewski, E., Nowacki, W., Rymarz, Cz., Wlodarczyk, E., "A Survey of the Scientific Activity of Sylwester Kaliski in the Coupled Fields Theory," ADVANCES IN MECHANICS, Vol 10, No 1, 1987.

2. Komarov, V. A., "Kvazistatsionarnoye elektromagnitoakusticheskoye preobrazovaniye v metallakh. (Osnovy teorii i primeneniye pri nerazrushayushchikh ispytaniyakh)" [Quasisteady Electromagneto-acoustic Conversion in Metals. (Principles of the Theory and Application in Nondestructive Testing)], Sverdlovsk, Ural Science Center, USSR Academy of Sciences, 1986, 235 pp.

3. Ambartsumyan, S. A., Bagdasaryan, G. Ye., Belubekyan, M. V., "Magnitouprugost' tonkikh obolochek i plastin" [Magnetoelasticity of Thin Shells and Plates], Moscow, Nauka, 1977, 272 pp.

4. Nowacki, W., "Elasticity Theory," Moscow, Mir, 1975.

5. Dolbin, N. I., "Propagation of Elastic Surface Waves in a Half-Space Located in a Magnetic Field," PRIKLADNAYA MATEMATIKA I TEORETICHESKAYA FIZIKA, No 1, 1963.

6. Bagdasaryan, G. Ye., Danoyan, Z. N., "Rayleigh Surface Magneto-acoustic Waves" in: "Mekhanika: Mezhvuzovskiy sbornik" [Mechanics: Interinstitutional Collection], Yerevan State University, No 2, 1982.

7. Danoyan, Z. N., Simonyan, A. N., "Rayleigh Surface Magnetoelastic Waves in the Presence of a Transverse Magnetic Field," IZVESTIYA AKADEMII NAUK ARMYANSKOY SSR: SERIYA MEKHANIKA, Vol 38, No 3, 1985.

UDC 539.1

# Diffraction of Shock Wave Around Wall Making Obtuse Angle

917F0082B IZVESTIYA AKADEMII NAUK ARMYANSKOY SSR: SERIYA MEKHANIKA in Russian Vol 43 No 1, 1990 (manuscript received 10 May 88) pp 10-18

[Article by L. D. Azatyan and A. G. Bagdoyev, Institute of Mechanics, ArmSSR Academy of Sciences]

[Text] The paper considers the problem of diffraction of a strong shock wave around an elastic wall that forms an oblique angle. Lighthill used Chaplygin transformation to study the analogous problem and get an analytical solution in the case of a solid wall [2].

## §1. Formulation of the Boundary Value Problem

Let a shock wave front move at velocity $U_0$ through a quiescent gas and impact at time $t \neq 0$ on a corner with sides that form a small angle $\varepsilon$ with a break. Fig. 1 shows the pattern of motion for some $t \neq 0$. The

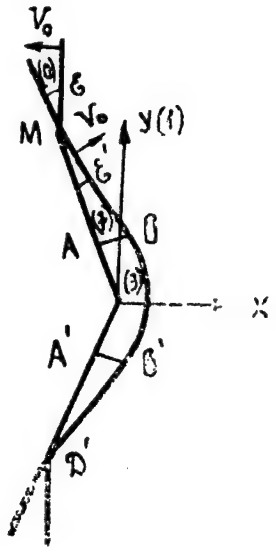


Fig. 1

parameters of homogeneous flow (1) behind the incident shock wave are determined from conditions of dynamic consistency [1]

$$P_1 = \frac{1}{\gamma(\gamma+1)} \frac{2\gamma M^2 - (\gamma-1)}{M^2} \rho_0 U_0^2$$

$$\rho_1 = \frac{(\gamma+1)M^2}{(\gamma-1)M^2+2} \rho_0, \quad q_1 = \frac{2}{\gamma-1} \frac{(M^2-1)}{M^2} U_0 \qquad (1.1)$$

(designation of parameters is conventional).

Let us determine the flow in region (2) behind the reflected shock wave. In the case of an elastic wall, assuming that motion in the wall is homogeneous, we get in the elastic region

$$\frac{\partial^2 w}{\partial x^2} = \frac{1}{a^2} \frac{\partial^2 w}{\partial t^2} = \frac{\rho_{CT}}{\lambda+2\mu} \frac{\partial^2 w}{\partial t^2}$$

where $\lambda$, $\mu$ are the elastic Lamé constants, $\rho_{CT}$ is the density of the elastic body, w is normal displacement of the elastic medium, and a is the velocity of propagation of the elastic longitudinal wave. On boundary x = 0 from the condition of concomitant motion of the wall and nearby particles of fluid (gas) we have

$$q_{2n} = \frac{\partial w}{\partial t} = af'(at)$$

where n is the normal to the wall, and the solution in the elastic region is w = f(x + at). Writing the conditions of continuity

$$\sigma_{xx}|_{x=0} = -P_2, \quad \sigma_{xx}|_{x=0} = \left(\lambda \frac{\partial w}{\partial x} + 2\mu \frac{\partial w}{\partial x}\right)\Big|_{x=0} = \rho_{CT} a^2 f'(at)$$

we can get two conditions on the wall

$$q_{2n} = af'(at), \quad \rho_{CT} a^2 f'(at) = -P_2$$

whence we have

$$q_{2n} = -\frac{P_2}{\rho_{CT} a} = -\frac{\theta P_2}{\rho_2 c_2} \qquad (1.2)$$

where $\theta = \rho_2 c_2 / \rho_{CT} a$.

Thus, accounting for a one-dimensional model in an elastic medium gives a boundary condition in the form of a Winkler base. Flow parameters in region (2) are determined from relations for an oblique shock wave [1]. Eliminating $P_2$, $\rho_2$ from these expressions, with allowance for (1.2), we find a cubic equation in order $\varepsilon$ for determining the normal velocity $V_o$ of the reflected shock

$$2\alpha\rho_1^2(\alpha P_1-q_1)V_0^3+2\rho_1(\alpha P_1-q_1)(1+3\alpha\rho_1 q_1)V_0^2+[(\gamma-3)\rho_1 q_1^2+$$
$$+6\alpha\rho_1^2 q_1^2(\alpha P_1-q_1)+2\alpha\rho_1 q_1 P_1-(\gamma-1)\alpha^2\rho_1 P_1^2]V_0-2\gamma P_1(\alpha P_1-q_1)+(\gamma-1)\rho_1 q_1^3-$$
$$-2\alpha\rho_1^2 q_1^4+2\alpha^2\rho_1^2 q_1^3 P_1-(\gamma-1)\alpha^2\rho_1 q_1 P_1^2=0, \quad \alpha=\theta/\rho_2 c_2 \tag{1.3}$$

Then in the same approximation from expressions for an oblique shock wave we get the values of the remaining parameters for a plane reflected shock

$$P_2=\frac{P_1+\rho_1 q_1(q_1+V_0)}{1+\alpha\rho_1(q_1+V_0)}, \quad \rho_2=\frac{\rho_1(q_1+V_0)[1+\alpha\rho_1(q_1+V_0)]}{\alpha P_1+\alpha\rho_1(q_1+V_0)^2+V_0}$$
$$q_{2x}=q_1(\varepsilon+\varepsilon'), \quad c_2=\left(\frac{\gamma P_2}{\rho_2}\right)^{1/2} \tag{1.4}$$

where $\varepsilon'$ is the angle of reflection determined from the condition of inseparability of the incident and reflected shock waves at point M

$$\varepsilon'=\frac{\varepsilon V_0}{U_0} \tag{1.5}$$

In the region of nonuniform flow (3), we will give all quantities the subscript "3." The boundary conditions of diffraction are: arcs AB and A'B' that are the fronts of perturbations produced by small angle $\varepsilon$, wall AOA', and curved shock wave BCB' resulting from diffraction away from the vertex.

The problem is to determine the parameters of motion in region (3). Since angle $\varepsilon$ is small, quantities

$$P=\frac{P_3-P_2}{\rho_2 c_2}, \quad \rho=\rho_3-\rho_2, \quad \bar{q}(u, v)=\bar{q}_3-\bar{q}_2 \tag{1.6}$$

will be of order $\varepsilon$, and the theory of perturbations can be used to find these quantities. Since there is no characteristic dimension of length, the problem can be considered self-similar, and then the equations of gas dynamics after linearization with respect to $\varepsilon$ in variables

$$\xi=\frac{x-q_{2x}t}{c_2 t}, \quad \eta=\frac{y}{c_2 t}$$

are written as

$$\xi\frac{\partial u}{\partial\xi}+\eta\frac{\partial u}{\partial\eta}=\frac{\partial P}{\partial\xi}, \quad \xi\frac{\partial v}{\partial\xi}+\eta\frac{\partial v}{\partial\eta}=\frac{\partial P}{\partial\eta}, \quad \xi\frac{\partial P}{\partial\xi}+\eta\frac{\partial P}{\partial\eta}=\frac{\partial u}{\partial\xi}+\frac{\partial v}{\partial\eta} \tag{1.7}$$

On plane $\xi$, $\eta$, the diffracted shock wave BCB' and the wall AOA' can be approximated by straight-line segments BB' and AA' (Fig. 2).

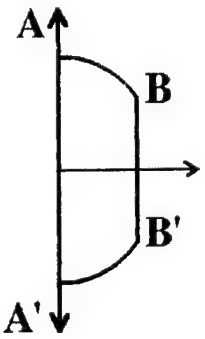


Fig. 2

In this context, the value of $\xi$ on the wall is equal to zero, and on the curved shock the value of $\xi$ is

$$\xi = \frac{V_0 - q_{2x}}{c_2} = k_0, \quad (k_0 < 1)$$

Arcs AB and A'B' in system $\xi$, $\eta$ coincide with the arc of a unit circle.

The solution of system (1.7) should satisfy the defined conditions on the boundary of the diffraction region. On perturbation fronts AB and A'B', the functions are continuous, and consequently on these arcs

$$P = 0, \quad \rho = 0, \quad \bar{q}(u, v) = 0 \tag{1.8}$$

According to (1.2), we have on the wall

$$q_{3x} = -\frac{\theta P_3}{\rho_2 c_2} = -\frac{\theta(P_2 + \rho_2 c_2 P)}{\rho_2 c_2} = -\frac{\theta P_2}{\rho_2 c_2} - \theta P$$

implying that on the wall in region (3)

$$d\theta = n$$

Then, as implied by the second equation of (1.7), at $\xi = 0$

$$\frac{\partial P}{\partial \xi} = -\theta \eta \frac{\partial P}{\partial \eta} \tag{1.9}$$

To find the boundary condition on $\xi = k_o$, we represent the perturbed shock wave front in the form $\xi = k_o + \psi(\eta)$, where $\psi(\eta)$ is a function that defines the unknown shape of the shock wave. Writing the conditions of dynamic consistency on the curved part of shock BB' and linearizing them relative to the flow behind the plane reflected wave, we get the following system of equations:

$$u_{12}-(\rho_2-\rho_1)V'+\rho(q_{2x}-V_0)=0,\quad \rho_2c_2P+2\rho_2u(q_{2x}-V_0)+\rho(q_{2x}-V_0)^2=0$$

$$q_1V'+uV_0-\frac{\gamma}{\gamma-1}c_2P+\frac{\gamma}{\gamma-1}\frac{P_2\rho}{\rho_2^2}-q_{2x}(u-V')=0 \tag{1.10}$$

$$v=-q_1\psi'-q_1(\varepsilon+\varepsilon')$$

where the projections on the normal and the tangent to the shock wave are written in the linear approximation in terms of projections on axes Ox, Oy, $V_o$ + V' is the velocity of the curved shock wave, V' = $c_2(\psi - \psi')$.

The solution of system (1.10) takes the form

$$P=Q(\psi-\eta_1\psi')/E,\quad u=G(\psi-\eta_1\psi')/E,\quad v=-q_1\psi'-q_1(\varepsilon+\varepsilon')$$

$$Q=\{(\rho_1-\rho_2)[2\gamma P_2+(\gamma-1)(q_{2x}-V_0)^2\rho_2]-(\gamma-1)(q_1+q_{2x})(q_{2x}-V_0)\rho_2^2\}(q-V_0) \tag{1.11}$$

$$G=\{(\gamma-1)(q_1+q_{2x})(q_{2x}-V_0)\rho_2^2-\gamma(\rho_1-\rho_2)[P_2+\rho_2(q_{2x}-V_0)^2]\}c_2$$

$$E=\rho_2[\gamma P_2-\rho_2(q_{2x}-V_0)^2]$$

Eliminating function $\psi$ from (1.11), we get

$$u=A_0P,\quad \eta\frac{\partial v}{\partial\eta}=B_0\frac{\partial P}{\partial\eta}\quad \text{on}\quad \xi=k_0 \tag{1.12}$$

where $A_o$ = G/Q, $B_o$ $q_1E/Q$.

Now by using equations (1.7) we can eliminate u and v from equations (1.12), giving the condition on the shock for P alone

$$\frac{\partial P/\partial\xi}{\partial P/\partial\eta}=\frac{\eta(A_0+k_0)-B_0k_0\eta^{-1}}{1-k_0^2} \tag{1.13}$$

In addition to condition (1.13), a condition is taken according to which the change in v along the shock from the center C to vertex B is

$$\int\frac{\partial v}{\partial\eta}d\eta=\int\frac{B_0}{\eta}\frac{\partial P}{\partial\eta}d\eta=q_{2x} \tag{1.14}$$

System (1.7) can be reduced to a single equation for P

$$\Delta P-\left(\xi\frac{\partial}{\partial\xi}+\eta\frac{\partial}{\partial\eta}+1\right)\left(\xi\frac{\partial P}{\partial\xi}+\eta\frac{\partial P}{\partial\eta}\right)=0 \tag{1.15}$$

The Chaplygin-Buseman transformation is used to solve the formulated boundary value problem with respect to the solution of equation (1.15) with boundary conditions (1.8), (1.9), (1.13), (1.14):

$$\xi = r\cos\vartheta, \quad \eta = r\sin\vartheta, \quad \left(r = \frac{2\rho}{1+\rho^2}, \quad \vartheta = \arctan\frac{\eta}{\xi}\right) \tag{1.16}$$

converting (1.5) to a Laplace equation in variables $\rho$, $\beta$. Then conformal mapping is used [2]:

$$z_1 = \ln\left(\frac{1+z}{1-z}\right) + \frac{1}{2}\pi i, \quad (z = \rho e^{i\beta}, \; z_1 = x_1 + iy_1) \tag{1.17}$$

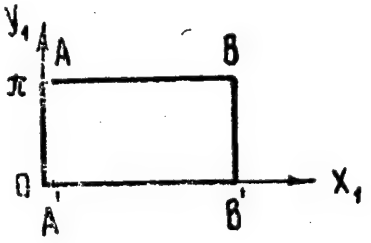


Fig. 3

Function (1.17) transforms diffraction region AA'B'B to a rectangle (Fig. 3)

$$0 \leqslant x_1 \leqslant b, \quad 0 \leqslant y_1 \leqslant \pi, \quad b = \frac{1}{2}\ln\frac{1+k_0}{1-k_0} \tag{1.18}$$

Thus, the problem is to determine the function P that satisfies the Laplace equation $\Delta P = 0$ in variables $x_1$, $y_1$ within rectangle (12.18), and the conditions:

$$\text{on } AB \text{ and } A'B' \text{ we have} \quad P = \frac{\partial P}{\partial x_1} = 0 \tag{1.19}$$

$$\text{on } AA': \; \frac{\partial P/\partial x_1}{\partial P/\partial y_1} = \theta\cot y_1 \tag{1.20}$$

$$\text{on } BB': \; -\frac{\partial P}{\partial x_1}\sin y_1\cos y_1 = \frac{\partial P}{\partial y_1}\left(A_0\cos^2 y_1 - B_0\frac{k_0}{(k_0')^2}\right), \quad k_0' = (1-k_0^2)^{1/2} \tag{1.21}$$

In virtue of equation (1.20), there is a difference between the given problem and the problem of [2] in which $\theta = 0$, while the fairly complex function $\omega(z_1) = \frac{\partial P}{\partial x_1} - i\frac{\partial P}{\partial y_1}$ is determined by trial and error.

## §2. Solution of Formulated Boundary Value Problem by Method of Separation of Variables

We will seek the solution of the Laplace equation $\Delta P = 0$ in the form [3]

$$P(x_1, y_1) = X(x_1)Y(y_1)$$

In this case we get

$$X=A\exp(\varkappa x_1)+B\exp(-\varkappa x_1),\quad Y=C\sin\varkappa y_1+D\cos\varkappa y_1$$

Satisfying condition (1.19), we get

$$P=\sum_{k=1}^{\infty}(A_k\exp(kx_1)+B_k\exp(-kx_1))\sin ky_1 \tag{2.1}$$

Condition (1.20) can be written as

$$\sum_{k=1}^{\infty}k[(A_k-B_k)\sin ky_1\sin y_1-\theta(A_k+B_k)\cos y_1\cos ky_1]=0 \tag{2.2}$$

and condition (1.21) can be written as

$$\sum_{k=1}^{\infty}k\left[(A_k\exp(k\lambda)-B_k\exp(-k\lambda))\sin ky_1\sin 2y_1+(A_k\exp(k\lambda)+B_k\exp(-k\lambda))\times\right.$$
$$\left.\times\left(A_0\cos 2y_1-A_0-B_0\frac{2k_0}{(k_0')^2}\right)\cos ky_1\right]=0 \tag{2.3}$$

Multiplying (2.2) and (2.3) by $\cos ly_1$ ($l = 0, 1, 2, \ldots$) and integrating from $-\pi$ to $\pi$, we get a system of equations for determining $A_k$ and $B_k$. It can be shown by simultaneous solution of these systems of equations that $A_k$ and $B_k$ with even k are equal to zero, while $A_k$ and $B_k$ for odd k will be determined from the following system of equations:

$$A_1(1-\theta)=B_1(1+\theta),\quad (1+\theta)A_1-(1-\theta)B_1=3[(1-\theta)A_3-(1+\theta)B_3]$$
$$(1+A_0)A_1e^{\lambda}-(1-A_0)B_1e^{-\lambda}+\frac{\pi}{2}(A_1e^{\lambda}+B_1e^{-\lambda})\left(A_0-2\frac{B_0k_0}{(k_0')^2}\right)=$$
$$+3[A_3(1+A_0)e^{3\lambda}-B_3(1-A_0)e^{-3\lambda}]=0 \tag{2.4}$$
$$A_{n+3}=[(1+\theta)(F-R)-(1-A_0)N\exp(-(n+3)\lambda)]/W$$
$$B_{n+3}=[(1-\theta)(F-R)-(1+A_0)N\exp((n+3)\lambda)]/W$$

where

$$F=(n-1)[(1-A_0)A_{n-1}\exp((n-1)\lambda)-(1+A_0)B_{n-1}\exp(-(n-1)\lambda)]$$
$$R=2(n+1)\left(A_0-2\frac{B_0k_0}{(k_0')^2}\right)(A_{n+1}\exp((n+1)\lambda)+B_{n+1}\exp(-(n+1)\lambda)]$$
$$N=(n+1)[(1+\theta)A_{n+1}-(1-\theta)B_{n+1}]$$
$$W=(n+3)[(1+A_0)(1+\theta)\exp((n+3)\lambda)-(1-A_0)(1-\theta)\exp(-(n+3)\lambda)]$$

From (2.4), all $A_k$ and $B_k$ are determined in terms of $A_1$ ($n > 2$). Condition (1.14) is used to find $A_1$. In what follows, $\bar{A}_k = A_k/A_1$, $\bar{B}_k = B_k/A_1$. The convergence of series (2.1) is proved as in [3].

## §3. Determination of Gas (Fluid) Flow Parameters in Diffraction Region

We write expression (2.1) for perturbed pressure in variables $\xi$, $\eta$. From formulas (1.15) and (1.17) we have

$$x_1=\frac{1}{2}\ln\frac{1+\xi}{1-\xi},\qquad y_1=\arctan\frac{\eta}{\sqrt{1-\xi^2-\eta^2}}+\pi i \tag{3.1}$$

With the use of (3.1), expression (2.1) in plane $\xi$, $\eta$ takes the form

$$P=\sum_{n=0}^{\infty}\left|A_{2n+1}\left(\frac{1+\xi}{1-\xi}\right)^{\frac{2n+1}{2}}+B_{2n+1}\left(\frac{1-\xi}{1+\xi}\right)^{\frac{2n+1}{2}}\right|\times$$
$$\times\sin\left|(2n+1)\frac{\pi}{2}+(2n+1)\arctan\frac{\eta}{\sqrt{1-\xi^2-\eta^2}}\right| \tag{3.2}$$

Components u and v can be determined from the equations of system (1.7). To find coefficient $A_1$, we find component v on $\xi = 0$ from the third equation of system (1.7)

$$v=\int\frac{1}{\eta}\frac{\partial P}{\partial\eta}d\eta=\sum_{n=0}^{\infty}(-1)^{n+1}(2n+1)(A_{2n+1}+B_{2n+1})\times$$
$$\times\left[\arcsin\eta+\sum_{k=1}^{\infty}\frac{1}{k}\sin(2k\arcsin\eta)\right] \tag{3.3}$$

The quantity v at $\xi = 0$, $\eta = 0$ is equal to the value of $q_{2\tau}$, and hence

$$A_1\sum_{n=0}^{\infty}(-1)^{n+1}(2n+1)(\bar{A}_{2n+1}+\bar{B}_{2n+1})\frac{\pi}{2}=q_{2\tau}$$

where $q_{2\tau}$ is determined from formula (1.4). Hence we have

| | $M=1,2$ | | | $M=1,6$ | | | $M=2$ | | |
|---|---|---|---|---|---|---|---|---|---|
| | $\theta=0$ | $\theta=0,1$ | $\theta=0,3$ | $\theta=0$ | $\theta=0,1$ | $\theta=0,3$ | $\theta=0$ | $\theta=0,1$ | $\theta=0,3$ |
| $\bar{P}(1)$ | 0 | 0 | 0 | 0 | 0 | 0 | 0 | 0 | 0 |
| $\bar{P}(0,5)$ | 0,24 | 0,21 | 0,16 | 0,41 | 0,36 | 0,31 | 0,49 | 0,43 | 0,37 |
| $P(0)$ | 0,28 | 0,25 | 0,21 | 0,48 | 0,44 | 0,40 | 0,58 | 0,52 | 0,47 |
| $\bar{P}(-0,5)$ | 0,24 | 0,21 | 0,16 | 0,41 | 0,36 | 0,31 | 0,48 | 0,43 | 0,37 |
| $P(-1)$ | 0 | 0 | 0 | 0 | 0 | 0 | 0 | 0 | 0 |
| $P_3(1)$ | 1,11 | 1,05 | 0,94 | 1,92 | 1,85 | 1,74 | 2,68 | 2,61 | 2,49 |
| $P_3(0,5)$ | 1,07 | 1,01 | 0,91 | 1,79 | 1,73 | 1,65 | 2,50 | 2,45 | 2,36 |
| $P_3(0)$ | 1,05 | 1,00 | 0,90 | 1,78 | 1,72 | 1,64 | 2,46 | 2,41 | 2,32 |
| $P_3(-0,5)$ | 1,07 | 1,01 | 0,91 | 1,79 | 1,73 | 1,65 | 2,50 | 2,45 | 2,36 |
| $P_3(-1)$ | 1,11 | 1,05 | 0,94 | 1,92 | 1,85 | 1,74 | 2,68 | 2,61 | 2,49 |

$$A_1 = \frac{2q_{2\pi}}{\sum_{n=0}^{\infty} (-1)^{n+1}(2n+1)\pi(\bar{A}_{2n+1} + \bar{B}_{2n+1})}$$

Numerical calculations are given to clarify the qualitative picture of reflection of a shock wave from the wall. From formula (3.2), the pressure on the wall is computed at Mach numbers $M = V_0/c_0 = 1.2, 1.6, 2$ and $\theta = 0, 0.1, 0.3$. Calculations for the distribution of dimensionless pressure $\tilde{P} = -P/\varepsilon U_0$ on the wall show that the pattern that occurs for a rigid wall is qualitatively retained, and moreover there is a decline in pressure $\tilde{P}$ with decreasing $\theta$. The distribution of total pressure $P_3$ on the wall is also calculated for $\varepsilon = 0.1$, pressure $P_3$ decreasing with increasing pressure $\theta$. The table also shows that $\tilde{P}$ and $P_3$ on the wall in the diffraction region increase with an increase in the Mach number at fixed $\theta$.

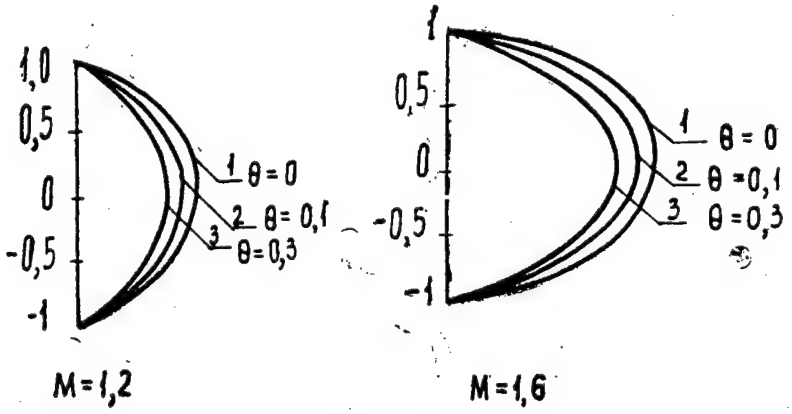


Fig. 4

Fig. 4 shows graphs of the distribution of pressure $\tilde{P}$ on the wall for two cases.

REFERENCES


1. Mieses, R, Karman, T, eds., "Problems of Mechanics. A Collection of Papers," Moscow, Izd-vo inostrannoy literatury, 1955, pp 573-578.

2. Lighthill, M. J., "The Diffraction of Blast" in: "Proceedings of the Royal Society of London. Series A: Mathematical and Physical Sciences," Vol 200, 1930.

3. Zhigalko, Ye. F., "Near-Normal Shock Wave Reflection in Linear Approximation," VESTNIK LENINGRADSKOGO GOSUDARSTVENNOGO UNIVERSITETA, No 13, Issue 3, 1970.

UDC 539.3

# Frequencies of Free Oscillations of Transversely Loaded Plates

917F0082C IZVESTIYA AKADEMII NAUK ARMYANSKOY SSR: SERIYA MEKHANIKA in Russian Vol 43 No 1, 1990 (manuscript received 19 Dec 88) pp 27-31

[Article by V. Ts. Gnuni, Institute of Mechanics, ArmSSR Academy of Sciences]

[Text] In the linear theory of bending of plates under a transverse load, it is known that forces $T_{ik}$ (i, k = 1, 2) do not arise in the middle plane of the plate, and hence it is assumed that the transverse load acting on the plate does not affect frequencies of free oscillations. However, in bending of very thin (flexible) plates, considerable tensile and shear forces arise in the middle plane of the plate for flexures comparable with the thickness of the plate, and these forces may significantly alter the frequencies of free oscillations of the plate.

This paper attempts to give a qualitative picture of the influence of transverse loading on the frequencies of free oscillations of a plate.

*1.* Let a flexible rectangular plate of dimensions a, b, h be hinged around the edge and subjected to the action of a uniform transverse load of intensity g.

The equations of bending of a flexible plate referenced to a rectangular cartesian coordinate system Oxyz are [1]

$$\begin{aligned} &\frac{1}{Eh}\Delta^2\Phi_0 + \frac{\partial^2 w_0}{\partial x^2}\frac{\partial^2 w_0}{\partial y^2} - \left(\frac{\partial^2 w_0}{\partial x \partial y}\right)^2 = 0 \\ &D\Delta^2 w_0 - \frac{\partial^2 w_0}{\partial x^2}\frac{\partial^2 \Phi_0}{\partial y^2} + 2\frac{\partial^2 w_0}{\partial x \partial y}\frac{\partial^2 \Phi_0}{\partial x \partial y} - \frac{\partial^2 w_0}{\partial y^2}\frac{\partial^2 \Phi_0}{\partial x^2} = q \end{aligned} \qquad (1.1)$$

where $w_0$, $\Phi_0$ are functions of flexure and forces of the initial static state, $D = EH^3/12(1 - \nu^2)$, E is Young's modulus, $\nu$ is Poisson's ratio.

The forces in the middle plane are defined as follows in terms of function $\Phi_0$:

$$T_{11}^0=\frac{\partial^2\Phi_0}{\partial y^2},\quad T_{22}^0=\frac{\partial^2\Phi_0}{\partial x^2},\quad T_{12}^0=-\frac{\partial^2\Phi_0}{\partial x\,\partial y} \tag{1.2}$$

Small transverse oscillations of the plate about the bent equilibrium state (1.1) are described by the equations [2]

$$\begin{aligned}&\frac{1}{Eh}\Delta^2\Phi+\frac{\partial^2 w_0}{\partial y^2}\frac{\partial^2 w}{\partial x^2}+\frac{\partial^2 w_0}{\partial x^2}\frac{\partial^2 w}{\partial y^2}-2\frac{\partial^2 w_0}{\partial x\,\partial y}\frac{\partial^2 w}{\partial x\,\partial y}=0\\&\rho h\frac{\partial^2 w}{\partial t^2}+D\Delta^2 w-T_{11}^0\frac{\partial^2 w}{\partial x^2}-2T_{12}^0\frac{\partial^2 w}{\partial x\,\partial y}-T_{22}^0\frac{\partial^2 w}{\partial y^2}-\\&-\frac{\partial^2 w_0}{\partial y^2}\frac{\partial^2\Phi}{\partial x^2}+2\frac{\partial^2 w_0}{\partial x\,\partial y}\frac{\partial^2 w}{\partial x\,\partial y}-\frac{\partial^2 w_0}{\partial x^2}\frac{\partial^2\Phi}{\partial y^2}=0\end{aligned} \tag{1.3}$$

where w, $\Phi$ are the functions of flexure and forces of the perturbed (oscillatory) state, $\rho$ is density of the plate material, and t is time.

Equations (1.3) account for both the forces $T_{ik}^0$ and flexures $w_0$ of the initial state.

Equations

$$\Phi_0=\Phi_{011}\sin\lambda_1 x\sin\mu_1 y,\quad w_0=f_{011}\sin\lambda_1 x\sin\mu_1 y \tag{1.4}$$

$$\Phi=\Phi_{mn}\sin\lambda_m x\sin\mu_n y\cos\omega_{mn}t,\quad w=f_{mn}\sin\lambda_m x\sin\mu_n y\cos\omega_{mn}t \tag{1.5}$$

where $\lambda_m = m\pi/a$, $\mu_n = n\pi/b$ identically satisfy the boundary conditions for hinged support of a plate

$$\begin{aligned}&T_{11}=0,\quad v=0,\quad w=0,\quad M_{11}=0\quad\text{for}\quad x=0,\ x=a\\&T_{22}=0,\quad u=0,\quad w=0,\quad M_{22}=0\quad\text{for}\quad y=0,\ y=b\end{aligned} \tag{1.6}$$

As shown in [1], expression (1.4) within the limits of flexures of initial state $w_0$ of the order of two or three plate thicknesses gives a rather good description of the initial bent state.

For (1.4), (1.5), using the Bubnov-Galerkin method, systems of equations (1.1), (1.3) yield

$$K_{11}f_{011}+d_{11}f_{011}^3=\frac{16}{\pi^2}q \tag{1.7}$$

$$\omega_{mn}=\omega_{0mn}\left(1+\frac{d_{mn}}{K_{mn}}f_0^2\right)^{1/2} \tag{1.8}$$

Here we have introduced the notation $\omega_{mn}$ to denote the frequencies of free oscillations of the plate about the bent equilibrium position, and

$$\omega_{0mn}=\sqrt{\frac{D}{\rho h}}(\lambda_m^2+\mu_n^2) \tag{1.9}$$

to denote the frequencies of free oscillations of the loaded plate

$$K_{mn}=D(\lambda_m^2+\mu_n^2)^2,\quad d_{mn}=\frac{Eh}{3}\left|\frac{\beta_{11}}{2(\lambda_1^2-\mu_1^2)^2}+\frac{\beta_{mn}}{(\lambda_m^2+\mu_n^2)^2}\right|\beta_{mn} \tag{1.10}$$

$$\beta_{mn}=\frac{32}{\pi^2}\frac{m^2n^2}{(4m^2-1)(4n^2-1)}\left|2mn\left(\frac{\lambda_1\mu_n}{\mu_1\lambda_m}+\frac{\mu_1\lambda_m}{\lambda_1\mu_n}\right)-1\right|$$

As can be seen from (1.8), the frequencies of free oscillations of a plate loaded by pressure q increase as compared with a plate free of pressure, and clearly the influence of the initial state can be disregarded for flexures of the initial state that are much less than the thickness.

2. By way of illustration, consider the example of a plate of square planform at $\nu = 0.3$. In this case, equation (1.7) is written as

$$f_*^3+2{,}51f_*-q_*=0 \tag{2.1}$$

where $f_* = f_{011}/h$, $q_* = 9a^4q/8\pi^2h^4E$ are dimensionless parameters of deflection and loading.

TABLE 1

| $q_*$ | 1 | 2 | 3 | 4 | 5 | 10 | 15 | 20 |
|---|---|---|---|---|---|---|---|---|
| $f_*$ | 0.37 | 0.67 | 0.90 | 1.1 | 1.2 | 1.8 | 2.1 | 2.4 |

Table 1 gives values of $f_*$ for several values of $q_*$.

From (1.8) for frequencies of free oscillations of a loaded square plate at $\nu = 0.3$ we have

$$\omega_{mn}=3\frac{h}{a^2}\sqrt{\frac{E}{\rho}}\left[(m^2+n^2)^2-0{,}2(1+3\alpha_{mn})\alpha_{mn}f_*^2\right]^{1/2} \tag{2.2}$$

where we have introduced the notation

$$\alpha_{mn}=\frac{m^2n^2(m^2+n^2-0{,}5)}{(m^2-0{,}25)(n^2-0{,}25)}$$

On the basis of (2.2) for various values of $q_*$ we determine the normalized frequencies of free oscillations of a loaded plate:

$$\omega_{*mn}=\frac{a^2}{3h}\sqrt{\frac{\rho}{E}}\,\omega_{mn} \tag{2.3}$$

for m = n = 1 for which $\omega_{mn} \longrightarrow \min_{m,n}$.

TABLE 2

| $q_*$ | 0 | 1 | 2 | 3 | 4 | 5 | 10 | 15 | 20 |
|---|---|---|---|---|---|---|---|---|---|
| $\omega_{11}^*$ | 2 | 2,6 | 3,3 | 3,9 | 4,6 | 5,2 | 7,1 | 8,4 | 9,3 |

Clearly, accounting for forces and flexures of the initial state has a fundamental effect on the frequencies of free oscillations of the loaded plate for flexures comparable with thickness.

The numerical results obtained in section 2 are general for arbitrary plates of square planform. However, it can easily be shown that these results are competent only for sufficiently thin plates that allow bending comparable with the thickness of the plate within the limits of elasticity or up to brittle fracture. From the condition

$$\sigma_{11}^2 - \sigma_{11}\sigma_{22} + \sigma_{22}^2 + 3\sigma_{12}^2 \leqslant \sigma_{adm}^2 \tag{2.4}$$

where fundamental stresses $\sigma^{11}$, $\sigma_{22}$, $\sigma_{12}$ are defined by formulas [1]

$$\sigma_{11} = \frac{1}{h}\frac{\partial^2\Phi_0}{\partial y^2} - \frac{Ez}{1-\nu^2}\left(\frac{\partial^2 w_0}{\partial x^2} + \nu\frac{\partial^2 w_0}{\partial y^2}\right)$$

$$\sigma_{22} = \frac{1}{h}\frac{\partial^2\Phi_0}{\partial x^2} - \frac{Ez}{1-\nu^2}\left(\frac{\partial^2 w_0}{\partial y^2} + \nu\frac{\partial^2 w_0}{\partial x^2}\right), \quad \sigma_{12} = -\frac{1}{h}\frac{\partial^2\Phi_0}{\partial x\,\partial y} - \frac{Ez}{1+\nu}\frac{\partial^2 w}{\partial x\,\partial y}$$

we can get the following estimate for the admissible relative thickness h/a:

$$\frac{h}{a} \leqslant \sqrt{\frac{2\sigma_{adm}}{E}}(14{,}1f_* - 0{,}889f_*^2)^{-1/2}$$

Here $f_*$ for prescribed q is determined from equation (2.1).

Thus, for prescribed a, E, $\sigma_{adm}$, there are real plates for which accounting for the initial state is significant in determining the frequencies of free oscillations. For example, at $\sigma_{adm}/E = 0.005$ and $f_* = 2.1$, $a = 200$ cm, we get $h \leqslant 2.53$ cm. Let us note that $f_* = 2.1$ corresponds to a normalized load of $q_* = 15$.

In conclusion, we note that questions of the influence of an external statically applied load on the frequencies of free oscillations have been rather thoroughly studied. And in the case of shells, the initial state caused by external loads may be treated as zero-torque [3] or significantly torqued, as well as nonlinear [2, 4]. On the other hand, in the case of plates, only geometric nonlinearity enables accounting for the effect of the initial state on frequencies of small oscillations

about the bent equilibrium state. In this sense, we can derive relations for studying the frequencies of free oscillations of plates of rectangular planform and for circular plates loaded by transverse pressure from the results of [2, 4] obtained for a cylindrical panel [2] and for corrugated shells of revolution [4].

Let us also note that we can derive an approximate analytical expression on the basis of [2] for the frequency of free oscillations of a loaded plate, and [4] can be a basis for exact numerical analysis of frequencies of a circular pressure-loaded plate.

REFERENCES


1. Volmir, A. S., "Gibkiye plastiny i obolochki" [Flexible Plates and Shells], Moscow, Gostekhizdat, 1956, 419 pp.

2. Gnuni, V. Ts., "Free Oscillations of Cylindrical Panel Loaded by External Pressure," INZHENERNYY ZHURNAL MEKHANIKA TVERDOGO TELA, No 2, 1968, pp 127-130.

3. Bolotin, V. V., "Dinamicheskaya ustoychivost' uprugikh sistem" [Dynamic Stability of Elastic Systems], Moscow, Gostekhizdat, 1956, 600 pp.

4. Naraykin, O. S., Ivanov, I. P., "Numerical Calculation of Free Oscillations of Preloaded Corrugated Shells of Revolution," IZVESTIYA VYSSHIKH UCHEBNYKH ZAVEDENIY: MASHINOSTROYENIYE, No 2, 1986, pp 42-46.

UDC 539.3

# Design of Optimum Circular Plate of Maximum Stiffness Made of Composite Material

917F0082D IZVESTIYA AKADEMII NAUK ARMYANSKOY SSR: SERIYA MEKHANIKA in Russian Vol 43 No 1, 1990 (manuscript received 13 Oct 88) pp 32-35

[Article by S. A. Grigoryan, Institute of Mechanics, ArmSSR Academy of Sciences]

[Text] Consider the problem of designing an orthotropic circular plate of radius R and thickness h under constant normal load q.

The plate is referenced to a cylindrical coordinate system 0, r, $\theta$, z so that coordinate plane z = 0 coincides with the middle plane of the plate. The material of the plate has three planes of elastic symmetry that are perpendicular at each point to the corresponding coordinate lines, the pole of anisotropy coinciding with the center of the plate. The plate of greatest stiffness is determined by varying the structure of the material and the location of the support contour.

It is assumed that the plate is made up of 2n layers alternately reinforced in the radial and circular directions. In this arrangement, the layers with odd numbering (1, 3,..., 2n-1) are made up of $m_1$ elementary layers that are reinforced in the radial direction, while the layers with even numbering (2, 4,..., 2n) are made up of $m_2$ elementary layers reinforced in the circular direction. From the foregoing we see that the total thickness is $h = nm\delta_o$, where $\delta_o$ is the thickness of a monolayer, and $m = m_1 + m_2$. The parameter $\xi = m_1/m$ defines the relative thickness of the radially reinforced layers of the stacked plate. It is assumed that elementary layers reinforced in both the radial and circular directions have the same content of reinforcing material per unit of volume, so that the elastic characteristics of these layers in orthogonal directions are the same [1].

Let the plate be supported around line $r = R_1$, where $0 < R_1 \leq R$. The equation of equilibrium of an orthotropic plate relative to bending W(r) is represented as [2]

$$D_{rr}\frac{d^4W_i}{dr^4}-2D_{rr}\frac{1}{r}\frac{d^3W_i}{dr^3}-D_{\theta\theta}\frac{1}{r^2}\cdot\frac{d^2W_i}{dr^2}+D_{\theta\theta}\frac{1}{r^3}\frac{dW_i}{dr}=q \qquad (1)$$

where i = 1, 2 for regions 0 ≦ r ≦ R and $R_1$ ≦ r ≦ R respectively.

Boundary conditions are written as

$$\lim_{r\to 0}W_1(r)<\infty,\quad \frac{dW_1}{dr}=0 \quad \text{for} \quad r=0$$

$$W_1=W_2=0,\quad \frac{dW_1}{dr}=\frac{dW_2}{dr},\quad M_{rr}^{(1)}=M_{rr}^{(2)} \quad \text{for} \quad r=R_1 \qquad (2)$$

$$M_{rr}^{(2)}=0,\quad N_r^{(2)}=0 \quad \text{for} \quad r=R$$

Here

$$M_{rr}^{(i)}=-D_{rr}\frac{d^2W_i}{dr^2}-D_{r\theta}\frac{1}{r}\frac{dW_i}{dr}$$

$$N_r^{(i)}=-D_{rr}\left(\frac{d^3W_i}{dr^3}+\frac{1}{r}\frac{d^2W_i}{dr^2}\right)+D_{\theta\theta}\frac{1}{r^2}\frac{dW_i}{dr} \qquad (3)$$

are the bending moment and the transverse force in cross sections r = const respectively, and $D_{rr}$, $D_{\theta\theta}$ and $D_{r\theta}$ are the stiffnesses of the plate of given structure [1]

$$D_{rr}=\frac{[(B_{rr}-B_{\theta\theta})\xi+B_{\theta\theta}]h^3}{12},\quad D_{\theta\theta}=\frac{[(B_{\theta\theta}-B_{rr})\xi+B_{rr}]h^3}{12},\quad D_{r\theta}=\frac{B_{r\theta}h^3}{12} \qquad (4)$$

Here $B_{rr}$, $B_{\theta\theta}$ and $B_{r\theta}$ are the elastic characteristics of a monolayer of orthotropic composite material.

In deriving these expressions, terms of order 1/n and $1/n^2$ were ignored, where n is the total number of monolayers reinforced in the radial and annular directions.

The solution of boundary value problem (1) and (2) with allowance for (3) takes the form

$$W_1=\frac{qR^4\cdot 12}{64B_{rr}h^3}\frac{32}{(1-\bar{B}_{rr})\xi+\bar{B}_{rr}}\left\{(\beta^{1+k}-\gamma^{1+k})\left[\frac{3+\mu}{(9-k^2)(1+k)(k+\mu)}+\right.\right.$$
$$\left.\left.+\frac{k(1+\mu)(\beta^{1-k}+\beta^{1+k}-2)+(k^2+\mu)(\beta^{1-k}-\beta^{1+k})}{2k(1-k^2)(1+k)(k+\mu)}\right]-(\beta^4-\gamma^4)\frac{1}{4(9-k^2)}\right\} \qquad (5)$$

$$W_2=\frac{qR^4\cdot 12}{64B_{rr}h^3}\frac{32}{(1-\bar{B}_{rr})\xi+\bar{B}_{rr}}\left\{\beta\gamma\left[\left(\frac{\gamma}{\beta}\right)^k-\left(\frac{\beta}{\gamma}\right)^k\right]\frac{1}{2k(1-k^2)}+\right.$$
$$+\frac{\beta^2-\gamma^2}{2(1-k^2)}+(\beta^{1+k}-\gamma^{1+k})\left[\frac{3+\mu}{(9-k^2)(1+k)(k+\mu)}+\right.$$
$$\left.\left.+\frac{k(1+\mu)(\beta^{1-k}+\beta^{1+k}-2)+(k^2+\mu)(\beta^{1-k}-\beta^{1+k})}{2k(1-k^2)(1+k)(k+\mu)}\right]\right\} \qquad (6)$$

where the notation

$$k^2 = \frac{D_{\theta\theta}}{D_{rr}} = \frac{(\bar{B}_{\theta\theta}-1)\xi+1}{(1-\bar{B}_{\theta\theta})\xi+\bar{B}_{\theta\theta}}, \quad \gamma = r/R, \quad \beta = R_1/R$$

$$\mu = \frac{D_{r\theta}}{D_{rr}} = \frac{\bar{B}_{r\theta}}{(1-\bar{B}_{\theta\theta})\xi+\bar{B}_{\theta\theta}}$$

has been introduced, in which $\bar{B}_{re} = B_{re}/B_{rr}$ and $\bar{B}_{ee} = B_{ee}/B_{rr}$.

Our problem is to find the optimum value of parameters $\xi$ and $\beta$ that maximize the stiffness of the plate, i.e.

$$W_{opt} = \min_{\xi,\beta} \max_{\gamma} W_1(\xi, \beta, \gamma) \tag{7}$$

with constraints

$$0 \leqslant \xi \leqslant 1, \quad 0 < \beta \leqslant 1, \quad 0 \leqslant \gamma \leqslant \beta \quad (i=1); \quad \beta \leqslant \gamma \leqslant 1 \quad (i=2) \tag{8}$$

and for assigned R, h, $B_{rr}$, $B_{ee}$, $B_{re}$ and q.

By way of example, consider a plate made up of monolayers of orthotropic boroplastic reinforced in the radial and annular directions.

An algorithm was developed for numerical solution of problem (7) with constraints (8), and the corresponding program was written.

| $\xi$ | $\beta$ | $\gamma$ | $\overline{W}$ |
|---|---|---|---|
| 0,00 | 0,693 | 1,00 | 0,6452 |
| 0,05 | 0,691 | 1,00 | 0,5463 |
| 0,10 | 0,689 | 1,00 | 0,4834 |
| 0,15 | 0,688 | 0,00 | 0,4325 |
| 0,20 | 0,687 | 0,00 | 0,3896 |
| 0,25 | 0,685 | 1,00 | 0,3688 |
| 0,30 | 0,684 | 1,00 | 0,3437 |
| 0,35 | 0,683 | 1,00 | 0,3235 |
| 0,40 | 0,682 | 1,00 | 0,3072 |
| 0,45 | 0,681 | 1,00 | 0,294 |
| 0,55 | 0,680 | 0,00 | 0,2674 |
| 0,60 | 0,679 | 0,00 | 0,2550 |
| 0,65 | 0,678 | 1,00 | 0,2486 |
| 0,70 | 0,677 | 1,00 | 0,2442 |
| 0,75 | 0,676 | 1,00 | 0,2410 |
| 0,80 | 0,676 | 0,00 | 0,2332 |
| 0,85 | 0,675 | 0,00 | 0,2262 |
| 0,90 | 0,674 | 0,00 | 0,2211 |
| 0,95 | 0,673 | 0,00 | 0,2195 |
| 1,00 | 0,672 | 0,00 | 0,2262 |

Values of $\beta_{opt} = \beta_*$, the value of $\gamma = r/R$ where $\max \overline{W}_1(\gamma, \beta, \xi)$ is reached, and the corresponding $\min_{\beta} \max_{\gamma} \overline{W}_1(\gamma, \beta, \xi)$ are given in the

table for several values of structure parameter $\xi$ characterizing the anisotropy of the plate. Here

$$\overline{W} = W \cdot 64 B_r h^3 / 12 q R^4$$

is is the dimensionless flexure of the plate.

As we see from the table, the optimum value of parameter $\beta$ that characterizes the position of the supporting edge for all values of structure parameter $\xi$ varies monotonically in the narrow range

$$0{,}672 \leqslant \beta \leqslant 0{,}693$$

The optimum plate design is realized for

$$\xi = 0{,}95, \quad \beta = 0{,}673 \quad \text{and here} \quad \overline{W}_{opt} = 0{,}2195$$

this design containing 5% of monolayers reinforced in annular directions. The worst design is realized for $\xi = 0$ (plate made up of monolayers reinforced only in the annular direction), and here

$$\max_{\xi} \min_{\beta} \max_{\gamma} \overline{W} = 0{,}6452$$

Thus, structural optimization leads to considerable improvement of the design of a plate in the sense of stiffness,

$$\max_{\xi} \min_{\beta} \max_{\gamma} \overline{W} = 2{,}94 \min_{\xi} \min_{\beta} \max_{\gamma} \overline{w}$$

i.e. roughly by a factor of 3.

REFERENCES


1. Belubkyan, E. V., Gnuni, V. Ts., "Designing a Flexible Circular Plate of Composite Material" in: "Inzhenernyye problemy stroitelnoy mekhaniki" [Engineering Problems of Structural Mechanics], Yerevan, 1985, pp 72-76.

2. Lekhnitskiy, S. G., "Anizotropnyye plastinki" [Anisotropic Plates], Moscow, OGIZ, 1947, 354 pp.

UDC 539.3

# Wave Propagation in Radially Inhomogeneous Elastic Ball

917F0082E IZVESTIYA AKADEMII NAUK ARMYANSKOY SSR: SERIYA MEKHANIKA in Russian Vol 43 No 1, 1990 (manuscript received 6 Feb 89) pp 36-43

[Article by S. G. Saakyan, Yerevan Polytechnic Institute imeni K. Marx]

[Text] The paper examines the axisymmetric problem of elastic wave propagation in a radially inhomogeneous elastic ball with the assumption that radial and tangential stresses on its surface are known. Standing oscillations of a radially inhomogeneous elastic ball are also studied.

*1. General formulas.* Let the Lamé coefficients $\lambda$, $\mu$ and density $\rho$ of an elastic ball be assigned in spherical coordinates $(r, \theta, \varphi)$ by functions

$$\lambda=\lambda_0\left(\frac{r}{r_0}\right)^{\frac{2\gamma}{\gamma-2}};\quad \mu=\mu_0\left(\frac{r}{r_0}\right)^{\frac{2\gamma}{\gamma-2}};\quad \rho=\rho_0\left(\frac{r}{r_0}\right)^{\frac{4}{\gamma-2}} \tag{1.1}$$

where $\lambda_0 = (\gamma - 2)\mu_0$; $\mu_0$, $\rho_0$ are the Lamé coefficients and density of the medium at $r = r_0$; $\gamma = (\lambda_0 + 2\mu_0)/\mu_0$.

The wave field of perturbations in an inhomogeneous elastic ball $r < r_0$ at any time $t > 0$ is determined by some equation of elasticity

$$(\lambda+2\mu)\operatorname{grad}\operatorname{div}\vec{u}-\mu\operatorname{curl}\operatorname{curl}\vec{u}+\operatorname{grad}\lambda\operatorname{div}\vec{u}+$$
$$+\operatorname{grad}\mu\times\operatorname{curl}\vec{u}+2\operatorname{grad}\mu\operatorname{grad}\vec{u}=\rho\frac{\partial^2\vec{u}}{\partial t^2} \tag{1.2}$$

under conditions

$$\vec{u}|_{t=0}=\left.\frac{\partial\vec{u}}{\partial t}\right|_{t=0}=0 \tag{1.3}$$

$$\sigma_{rr}(r_0, \theta, t)=\sigma_0 f_1(\theta, t);\ \sigma_{r\theta}(r_0, \theta, t)=\sigma_0 f_2(\theta, t);\ \sigma_{r\varphi}(r_0, \theta, t)=\sigma_0 f_3(\theta, t) \tag{1.4}$$

Assuming Rayleigh's hypothesis, according to which the relation between components of the stress tensor and displacement vector $\vec{u}(u_r, u_\theta, u_\varphi)$ of an inhomogeneous elastic medium is the same as for a homogeneous medium, we have in the axisymmetric case

$$\sigma_{rr}=\lambda\Theta+2\mu\frac{\partial u_r}{\partial r};\quad \sigma_{r\theta}=\mu\left(\frac{1}{r}\frac{\partial u_r}{\partial\theta}+\frac{\partial u_\theta}{\partial r}-\frac{u_\theta}{r}\right) \tag{1.5}$$

$$\sigma_{\theta\theta}=\lambda\Theta+2\mu\left(\frac{1}{r}\frac{\partial u_\theta}{\partial\theta}+\frac{u_r}{r}\right);\quad \sigma_{r\varphi}=\mu\left(\frac{\partial u_\varphi}{\partial r}-\frac{u_\varphi}{r}\right) \tag{1.6}$$

where

$$\sigma_{\varphi\varphi}=\lambda\Theta+2\mu\left(\frac{u_r}{r}+\frac{u_\theta}{r}\cot\theta\right);\quad \sigma_{\theta\varphi}=\mu\left(\frac{1}{r}\frac{\partial u_\varphi}{\partial\theta}-\frac{u_\varphi}{r}\cot\theta\right) \tag{1.7}$$

$$\Theta=\frac{1}{r^2}\frac{\partial}{\partial r}(r^2u_r)+\frac{1}{r\sin\theta}\frac{\partial}{\partial\theta}(\sin\theta u_\theta) \tag{1.8}$$

The displacement vector $\vec{u}$ of the radially inhomogeneous medium is represented in terms of generalized potentials as follows:

$$\vec{u}(r,\theta,t)=\operatorname{grad}\Phi_3(r,\theta,t)+\left(\frac{r}{r_0}\right)^{-\frac{1}{\gamma-2}}\operatorname{curl}\operatorname{curl}[\Phi_2(r,\theta,t)\vec{e}_r]+\operatorname{curl}[\Phi_3(r,\theta,t)\vec{e}_r] \tag{1.9}$$

i.e. the components of the displacement vector $\vec{u}$ are determined from the formulas

$$u_r=r_0\left[\frac{\partial\Phi_1^*}{\partial R}-R^{-\frac{2\gamma}{\gamma-2}}\frac{1}{\sin\theta}\frac{\partial}{\partial\theta}\left(\sin\theta\frac{\partial\Phi_2^*}{\partial\theta}\right)\right] \tag{1.10}$$

$$u_\theta=r_0\left[\frac{1}{R}\frac{\partial\Phi_1^*}{\partial R}+R^{-\frac{\gamma-2}{\gamma-2}}\frac{\partial^2\Phi_2^*}{\partial R\partial\theta}\right] \tag{1.11}$$

$$u_\varphi=-\frac{r_0}{R}\frac{\partial\Phi_3^*}{\partial\theta} \tag{1.12}$$

where $\vec{e}_r$ is the basis vector with respect to the r-axis, $R = r/r_0$, $\Phi_i^* = \Phi_i/r_0^2$, $i = 1, 2, 3$.

Then, representation (1.9) of the displacement vector permits separation of the vector equation of motion (1.2) into the following independent scalar equations [1]:

$$\Delta\Phi_1^*+\frac{4}{(\gamma-2)R}\frac{\partial\Phi_1^*}{\partial R}-\frac{4}{(\gamma-2)R^2}\Phi_1^*-\frac{1}{\gamma R^2}\frac{\partial^2\Phi_1^*}{\partial\tau^2}=0 \tag{1.13}$$

$$\Delta\Phi_2^*-\frac{2\gamma}{(\gamma-2)R}\frac{\partial\Phi_2^*}{\partial R}-\frac{4\gamma}{(\gamma-2)R^2}\Phi_2^*-\frac{1}{R^2}\frac{\partial^2\Phi_2^*}{\partial\tau^2}=0 \tag{1.14}$$

$$\Delta\Phi_3^*+\frac{4}{(\gamma-2)R}\frac{\partial\Phi_3^*}{\partial R}-\frac{\gamma}{(\gamma-2)R^2}\Phi_3^*-\frac{1}{R^2}\frac{\partial^2\Phi_3^*}{\partial\tau^2}=0 \tag{1.15}$$

where

$$\Delta \equiv \frac{1}{R^2}\frac{\partial}{\partial R}R^2\frac{\partial}{\partial R}+\frac{1}{R^2\sin\vartheta}\frac{\partial}{\partial\vartheta}\sin\vartheta\frac{\partial}{\partial\vartheta};\quad \tau=\sqrt{\frac{\mu_0}{\rho_0}}\frac{t}{r_0}$$

*2. Wave propagation in an inhomogeneous elastic ball when its surface is acted on by radial time-dependent pressures.* In this case, generalized potential $\Phi_1^*$ depends on R and $\tau$, $\Phi_2^* \equiv \Phi_3^* \equiv 0$. Wave propagation in the ball is described by the equation

$$\frac{\partial^2\Phi_1^*}{\partial R^2}+\frac{2\gamma}{(\gamma-2)R}\frac{\partial\Phi_1^*}{\partial R}-\frac{4}{(\gamma-2)R^2}\Phi_1^*-\frac{1}{\gamma R^2}\frac{\partial^2\Phi_1^*}{\partial\tau^2}=0 \qquad (2.1)$$

under conditions

$$\Phi_1^*|_{\tau=0}=\left.\frac{\partial\Phi_1}{\partial\tau}\right|_{\tau=0}=0 \qquad (2.2)$$

$$\left|\gamma R^{\frac{4\gamma}{\gamma-2}}\frac{\partial^2\Phi_1^*}{\partial R^2}+2(\gamma-2)R^{\frac{\gamma+2}{\gamma-2}}\frac{\partial\Phi_1^*}{\partial R}\right|_{R=1}=-\frac{\sigma_0}{\mu_0}f(\tau) \qquad (2.3)$$

Equation (2.1) and condition (2.3) in the Laplace transform with respect to $\tau$

$$\overline{\Phi}_1^*(R,p)=\int_0^\infty \Phi_1^*(R,\tau)\exp(-p\tau)d\tau \qquad (2.4)$$

are as follows:

$$\frac{d^2\overline{\Phi}_1^*}{dR^2}+\frac{2\gamma}{(\gamma-2)R}\frac{d\overline{\Phi}_1^*}{dR}-\left(\frac{p^2}{\gamma}+\frac{4}{\gamma-2}\right)\frac{\overline{\Phi}_1^*}{R^2}=0 \qquad (2.5)$$

$$\left|\gamma R^{\frac{4\gamma}{\gamma-2}}\frac{d^2\overline{\Phi}_1^*}{dR^2}+2(\gamma-2)R^{\frac{\gamma+2}{\gamma-2}}\frac{d\overline{\Phi}_1^*}{dR}\right|_{R=1}=-\frac{\sigma_0}{\mu_0}\overline{f}(p) \qquad (2.6)$$

The solution of Euler's equation (2.5) under condition (2.6), assuming boundedness in the center of the ball, takes the form

$$\overline{\Phi}_1^*(R,p)=-\frac{\sigma_0\overline{f}(p)R^{\alpha-c}}{\gamma\mu_0(\alpha-c)(\alpha-d)} \qquad (2.7)$$

where

$$c=\frac{\gamma+2}{2(\gamma-2)};\quad d=c-\frac{\gamma-4}{\gamma};\quad \alpha=\sqrt{\frac{p^2}{\gamma}+c^2+\frac{4}{\gamma-2}}$$

The radical branch $\alpha$ is fixed by the condition $\arg\alpha = 0$ for $p > 0$. According to (1.10)-(1.12) and (1.5)-(1.8), The components of the displacement vector and stress tensor take the form

$$\bar{u}_r(R, p) = -\frac{r_0 \sigma_0 \bar{f}(p) R^{\alpha + c_0 + 1}}{\gamma \mu_0 (\alpha - d)} \tag{2.8}$$

$$\bar{\sigma}_{rr}(R, p) = -\sigma_0 \bar{f}(p) R^{\alpha + c_0} \tag{2.9}$$

$$\bar{\sigma}_{\theta\theta}(R, p) = \bar{\sigma}_{\varphi\varphi}(R, p) = -\frac{\gamma - 2}{\gamma} \sigma_0 \bar{f}(p) \left(1 + \frac{b}{\alpha - d}\right) R^{\alpha + c_0} \tag{2.10}$$

where

$$c_0 = \frac{6 - \gamma}{2(\gamma - 2)}; \quad b = \frac{2(3\gamma - 4)}{\gamma(\gamma - 2)}$$

We get the inverse Fourier transform of images (2.8)-(2.10) under condition $\bar{f}(p) = 1$, i.e. $f(\tau) = \delta(\tau)$, where $\delta$ is the Dirac function. In the general case for any $\bar{f}(p)$, we find the inversion of expressions (2.8)-(2.10) from a convolution formula.

From formulas [2]

$$\exp(-a\sqrt{p^2 + b^2}) \doteq \delta(\tau - a) - H(\tau - a) \frac{ab}{\sqrt{\tau^2 - a^2}} J_1(b\sqrt{\tau^2 - a^2}) \tag{2.11}$$

$$\bar{f}(\sqrt{p^2 + b^2}) = f(\tau) - b \int_0^{\tau} f(\sqrt{\tau^2 - u^2}) J_1(bu)\, du$$

we get

$$u_r(R, \tau) = -\frac{r_0 \sigma_0}{\sqrt{\gamma}\, \mu_0} R^{c_0 + 1} H\left(\tau - \frac{\ln R^{-1}}{\sqrt{\gamma}}\right) \left\{ \exp\left[ -d\sqrt{\gamma}\left(\tau - \frac{\ln R^{-1}}{\sqrt{\gamma}}\right)\right] - \right.$$

$$\left. - R^{-\alpha} \int_0^{\sqrt{\tau^2 - \left(\frac{\ln R^{-1}}{\sqrt{\gamma}}\right)^2}} \exp[-d\sqrt{\gamma}\sqrt{\tau^2 - u^2}]\, J_1(\sqrt{\gamma}\, \sigma_0 u)\, du \right\} \tag{2.12}$$

$$\sigma_{rr}(R, \tau) = -\sigma_0 R^{c_0} \left\{ \delta\left(\tau - \frac{\ln R^{-1}}{\sqrt{\gamma}}\right) - \right.$$

$$\left. - \frac{\sigma_0 \ln R^{-1} H\left(\tau - \frac{\ln R^{-1}}{\sqrt{\gamma}}\right)}{\sqrt{\tau^2 - \left(\frac{\ln R^{-1}}{\sqrt{\gamma}}\right)^2}} J_1\left(\sigma_0 \sqrt{\gamma} \sqrt{\tau^2 - \left(\frac{\ln R^{-1}}{\sqrt{\gamma}}\right)^2}\right) \right\} \tag{2.13}$$

$$\sigma_{00}(R,\tau)=\sigma_{\varphi\varphi}(R,\tau)=-\frac{\gamma-2}{\gamma}\sigma_0 R^{\alpha_0}\left\{\delta\left(\tau-\frac{\ln R^{-1}}{\sqrt{\gamma}}\right)-\right.$$

$$-H\left(\tau-\frac{\ln R^{-1}}{\sqrt{\gamma}}\right)\left\{\frac{\alpha_0\ln R^{-1}}{\sqrt{\tau^2-\left(\frac{\ln R^{-1}}{\sqrt{\gamma}}\right)^2}}J_1\left(\alpha_0\sqrt{\gamma}\sqrt{\tau^2-\left(\frac{\ln R^{-1}}{\sqrt{\gamma}}\right)^2}\right)-\right.$$

$$-b\sqrt{\gamma}\exp\left[-d\sqrt{\gamma}\left(\tau-\frac{\ln R^{-1}}{\sqrt{\gamma}}\right)\right]-b\alpha_0\sqrt{\gamma}R^{-d}\int_0^{\sqrt{\tau^2-\left(\frac{\ln R^{-1}}{\sqrt{\gamma}}\right)^2}}\exp[-d\sqrt{\gamma}\sqrt{\tau^2-u^2}]\times$$

$$\left.\left.\times J_1(\alpha_0\sqrt{\gamma}u)du\right\}\right\} \qquad (2.14)$$

where H is the Heaviside function, $J_1$ is a Bessel function.

Waves of displacements and stresses propagate in a radially inhomogeneous elastic ball when its surface is acted on by pressures that depend only on time. The front of these waves at any $\tau > 0$ is defined by the equation

$$\tau-\frac{\ln R^{-1}}{\sqrt{\gamma}}=0 \qquad (2.15)$$

Equation (2.15) defines a sphere with radius $R = \exp(-\sqrt{\gamma}\tau)$. As a result of rapid decay of the radius of the wave front in time, the displacement and stress waves have an appreciable effect near the surface of the ball. These waves do not reach the center of the ball, and consequently no reflected waves originate from the center.

In formulas (2.12)-(2.14), the terms associated with the Heaviside function describe waves that do not originate in a homogeneous medium. It propagates with a wake, and its occurrence can be attributed to dispersion of transmitted waves in the inhomogeneous medium. Near front (2.15), the so-called wave with a wake has a finite discontinuity implied by formulas (2.12)-(2.14) if it be considered that the limit $z^{-1}J_1(bz)$ as $z \to 0$ is finite.

Let us consider steady-state waves in a radially inhomogeneous ball. For boundary condition $f(\tau) = \sigma_0 e^{i\omega\tau}$ we get

$$u_r(R,\tau)=-\frac{\gamma_0\sigma_0 R^{\alpha_0+1}\exp(i\Omega)}{\gamma\mu_0(\alpha-d)} \qquad (2.16)$$

where phase $\Omega$ is defined by the relation

$$\Omega=\omega\tau-\ln R^{-1}\sqrt{\frac{\omega^2}{\gamma}-c^2-\frac{1}{\gamma-2}} \qquad (2.17)$$

The phase velocity is determined from the condition $\Omega$ = const:

$$v_\varphi = \frac{d(1-R)}{d\tau} = \frac{\omega R}{\sqrt{\frac{\omega^2}{\gamma} - c^2 - \frac{4}{\gamma-2}}} \tag{2.18}$$

The wave number is

$$K(\omega) = \frac{\omega}{v_\varphi} = \frac{1}{R}\sqrt{\frac{\omega^2}{\gamma} - c^2 - \frac{4}{\gamma-2}} \tag{2.19}$$

For the group velocity we get the expression

$$v_g = \frac{d\omega}{dK} = \frac{R\gamma}{\omega}\sqrt{\frac{\omega^2}{\gamma} - c^2 - \frac{4}{\gamma-2}} \tag{2.20}$$

As we see from formulas (2.18) and (2.20), the phase and group velocities depend on frequency ω, coordinate R, and the quantity γ.

Standing waves appear in a radially inhomogeneous ball at frequencies lower than the limit

$$\omega^* = \sqrt{\gamma\left(c^2 + \frac{4}{\gamma-2}\right)} \tag{2.21}$$

*3. Resonant frequencies of a radially inhomogeneous elastic ball in the case of standing waves.* Consider the solution of system of equations (1.13)-(1.15), assuming that the generalized potentials take the form

$$\Phi_j^*(R, \vartheta, \tau) = \varphi_j(R) P_n(\cos\vartheta) e^{i\omega\tau}, \quad j = 1, 2, 3 \tag{3.1}$$

where $P_n \cos\theta$ is a Legendre function, and radial and tangential stresses on the surface of the ball are equal to zero.

Substituting (3.1) in (1.13)-(1.15) and (1.4), we have system of equations

$$\frac{d^2\varphi_1}{dR^2} + \frac{2\gamma}{(\gamma-2)R}\frac{d\varphi_1}{dR} - \left[n(n+1) + \frac{4}{\gamma-2} - \frac{\omega^2}{\gamma}\right]\frac{\varphi_1}{R^2} = 0 \tag{3.2}$$

$$\frac{d^2\varphi_2}{dR^2} - \frac{4}{(\gamma-2)R}\frac{d\varphi_2}{dR} - \left[n(n+1) + \frac{4\gamma}{\gamma-2} - \omega^2\right]\frac{\varphi_2}{R^2} = 0 \tag{3.3}$$

$$\frac{d^2\varphi_3}{dR^2} + \frac{2\gamma}{(\gamma-2)R}\frac{d\varphi_3}{dR} - \left[n(n+1) + \frac{\gamma}{\gamma-2} - \omega^2\right]\frac{\varphi_3}{R^2} = 0 \tag{3.4}$$

with boundary condition

$$\left\{\mu_0 R^{\frac{2\gamma}{\gamma-2}}\left[(\gamma-2)\Theta + 2\frac{\partial u_r}{\partial R}\right]\right\}_{R=1} = 0 \tag{3.5}$$

$$\left\{\mu_0 R^{\frac{2\gamma}{\gamma-2}}\left[\frac{1}{R}\frac{\partial u_r}{\partial\vartheta} + \frac{\partial u_\vartheta}{\partial R} + \frac{u_\vartheta}{R}\right]\right\}_{R=1} = 0 \tag{3.6}$$

$$\left\{\mu_0 R^{\frac{2\gamma}{\gamma-2}}\left[\frac{\partial u_\varphi}{\partial R} - \frac{u_\varphi}{R}\right]\right\}_{R=1} = 0 \tag{3.7}$$

where

$$u_r = r_0 \left| \frac{d\varphi_1}{dR} + n(n+1)R^{-\frac{2}{\gamma-2}}\varphi_2 \right| P_n(\cos\vartheta) \tag{3.8}$$

$$u_\vartheta = r_0 \left| \frac{\varphi_1}{R} - R^{-\frac{\gamma+2}{\gamma-2}} a\varphi_2 \right| \frac{dP_n(\cos\vartheta)}{d\vartheta} \tag{3.9}$$

$$u_\varphi = -\frac{r_0}{R}\varphi_3 \frac{dP_n(\cos\vartheta)}{d\vartheta} \tag{3.10}$$

The solution of Euler equations (3.2)-(3.4) under condition of boundedness in the center of the ball is as follows:

$$\varphi_1(R) = A_n R^{\gamma_n - c}; \quad \varphi_2(R) = B_n R^{\beta_n - c}; \quad \varphi_3(R) = C_n R^{\delta_n - c} \tag{3.11}$$

where $A_n$, $B_n$, $C_n$ are arbitrary constants,

$$\gamma_n = \sqrt{a_n^2 - \frac{\omega^2}{\gamma}}; \quad \beta_n = \sqrt{b_n^2 - \omega^2}; \quad \delta_n = \sqrt{c_n^2 - \omega^2}$$

Radial oscillations of an inhomogeneous elastic ball occur at n = 0. Solution (3.11) at n = 0 with boundary condition (3.5)-(3.7) gives the equation of frequencies

$$a_n^2 = n(n+1)c^2 + \frac{4}{\gamma}; \quad b_n^2 = n(n-1)c^2 + \frac{4\gamma}{\gamma-2}; \quad c_n^2 = n(n+1)c^2 + \frac{4}{\gamma-2}$$

The roots of equation (3.12) that define the resonant frequencies of radial oscillations are as follows:

$$(z_0 - c)(z_0 - d) = 0 \tag{3.12}$$

Roots of frequency equation $\Delta_n(\omega) = 0$

| $\gamma$ \ $n$ | 0 | 1 | 2 | 3 | 4 | 5 | 6 |
|---|---|---|---|---|---|---|---|
| 2,5 | 2,3665<br>4,4722 | 0,0016<br>2,8647<br>4,4722 | 1,2245<br>4,0385<br>4,4722 | 1,6942<br>4,4722<br>5,4739 | 2,2565<br>4,4722<br>6,9535 | 2,9270<br>4,4722<br>8,3666 | 3,6715<br>4,4722 |
| 3 | 2,5821<br>3,4642 | 2,5821<br>3,4642 | 0,0030<br>3,0817<br>3,4642 | 1,3040<br>3,4642<br>4,1854 | 1,9568<br>3,4642<br>5,4777 | 2,6994<br>3,4642 | 3,4642<br>3,5126 |
| 10 | 2,2362<br>3,2849 | 0,0033<br>2,2362<br>2,6439 | 1,4912<br>2,2362 | 2,2362<br>2,4089 | 2,2362<br>3,3412 | 2,2362<br>4,2849 | 2,2362<br>5,2334 |

$$\omega_{1p}=2\sqrt{\frac{\gamma}{\gamma-2}};\quad \omega_{2p}=2\sqrt{\frac{3\gamma-4}{\gamma}} \tag{3.13}$$

At n = 0, substituting (3.11) in boundary condition (3.5)-(3.7). we get a homogeneous system of linear algebraic equations relative to $A_n$, $B_n$, $C_n$. The condition under which the homogeneous system has a nontrivial solution is as follows:

$$\Delta_n(\omega)\equiv\{(\alpha_n-c)[\gamma(\alpha_n-c)+\gamma-4]-(\gamma-2)n(n+1)\}[(\beta_n+c)(\beta_n-c-2)+ \\ +n(n+1)]-4n(n+1)(\alpha_n-c-1)(\beta_n-c-3)=0 \tag{3.14}$$

The roots of equation (3.14) define the dimensionless resonant frequencies of a radially inhomogeneous elastic ball. They are given in the table for several values of n and $\gamma$.

REFERENCES


1. Saakyan, S. G., "Independent Scalar Equations of Motion of Some Radially Inhomogeneous Isotropic Elastic Media," DOKLADY AKADEMII NAUK ARMYANSKOY SSR, Vol 85, No 4, 1987.

2. Doetsch, G., "Handbook on Practical Application of Laplace and Z Transforms," Moscow, Nauka, 1971, 288 pp.

UDC 539.374

# Introduction of Rigid Cylinder Into Cylinder Made of Material Conforming to Power Hardening Law

917F0082F IZVESTIYA AKADEMII NAUK ARMYANSKOY SSR: SERIYA MEKHANIKA in Russian Vol 43 No 1, 1990 (manuscript received 1 Jun 88) pp 44-51

[Article by Zh. G. Apikyan, Institute of Mechanics, ArmSSR Academy of Sciences]

[Text] In [1-3], researchers consider introduction of a cylindrical solid into an ideally plastic tube (isotropic and orthotropic cases).

Our paper takes a look at introduction (internal and external) of a near cylindrical solid into a cylinder made of material with power-law hardening.

*1.* Let a cylindrical tube made of material taken as incompressible and power-law hardenable fit tightly in an absolutely rigid cylindrical mold. The inside and outside radii of the tube are *a* and *b* respectively. A cylindrical tube of considerably harder material with varying outside radius $R = R(z) = a + \nu u_1 \exp(\nu z/b)$, where $\nu$ and $u_1$ are prescribed positive constants (Fig. 1), is coaxially forced into this tube (internal introduction). The material of the second tube is taken as nondeformable.

The problem is solved in the cylindrical coordinate system $r, \theta, z$ fixed to the rigid tube so that plane $z = 0$ passes through the entrance end cross section, and the positive direction of the $Oz$ axis is opposite to the direction of motion along the axis of the tube. The end $z = l$ of the tube is assumed to be free of external forces. Then the components of displacement $u, w$ in directions $r, z$ do not depend on $\theta$, and $v = 0$.

The equations of equilibrium, relations between the components of strains, displacements and stresses, and the law of hardening take the form

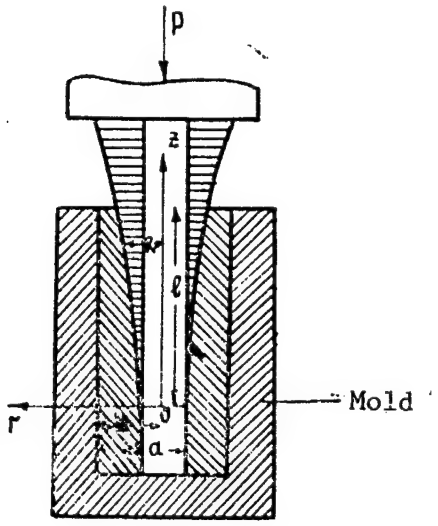


Fig. 1

$$\frac{\partial \sigma_r}{\partial r} + \frac{\partial \tau_{rz}}{\partial z} + \frac{\sigma_r - \sigma_\theta}{r} = 0, \qquad \frac{\partial \tau_{rz}}{\partial r} + \frac{\partial \sigma_z}{\partial z} + \frac{\tau_{rz}}{r} = 0 \tag{1.1}$$

$$\varepsilon_r = \frac{\partial u}{\partial r}, \quad \varepsilon_\theta = \frac{u}{r}, \quad \varepsilon_z = \frac{\partial w}{\partial z}, \quad \gamma_{rz} = \frac{1}{2}\left(\frac{\partial u}{\partial z} + \frac{\partial w}{\partial r}\right) \tag{1.2}$$

$$\sigma_r - \sigma = L\varepsilon_r, \quad \sigma_\theta - \sigma = L\varepsilon_\theta, \quad \sigma_z - \sigma = L\varepsilon_z, \quad \tau_{rz} = L\gamma_{rz}, \quad \sigma_i = k\varepsilon_i \tag{1.3}$$

where

$$\sigma_i = \frac{1}{\sqrt{2}}\sqrt{(\sigma_r - \sigma_\theta)^2 + (\sigma_\theta - \sigma_z)^2 + (\sigma_z - \sigma_r)^2 + 6\tau_{rz}^2}$$

$\varepsilon_i = \frac{2}{\sqrt{3}}\sqrt{\varepsilon_r^2 + \varepsilon_r\varepsilon_\theta + \varepsilon_\theta^2 + \gamma_{rz}^2}$ are intensities of stresses and strains,

$L = 2\sigma_i/(3\varepsilon_i)$, $\sigma = \frac{1}{3}(\sigma_r + \sigma_\theta + \sigma_z)$

We seek the components of displacements in the form

$$u = \lambda f \exp(\lambda z), \quad w = -\frac{\psi}{r}\exp(\lambda z) \tag{1.4}$$

where f = f(r), ψ = (rf)', λ is a constant, and the prime denotes the derivative with respect to r.

Then

$$\varepsilon_r = \lambda f' \exp(\lambda z), \quad \varepsilon_\theta = \frac{\lambda f}{r}\exp(\lambda z), \quad \varepsilon_z = -\frac{\lambda\psi}{r}\exp(\lambda z) \tag{1.5}$$

$$\gamma_{rz} = \frac{T}{2}\exp(\lambda z), \quad L = k_1 e_0^{\frac{m-1}{2}}\exp((m-1)\lambda z), \quad \varepsilon_i = \frac{2}{\sqrt{3}}\sqrt{e_0}\exp(\lambda z)$$

where

$$T=\lambda^2 f-\left(\frac{\psi}{r}\right)', \quad e_0=\lambda^2\left(f'^2+\frac{f^2}{r^2}+\frac{ff'}{r}\right)-\frac{T^2}{4}, \quad k_1=2^m 3^{-\frac{m+1}{2}} k$$

From relations (1.2) and (1.5) we get

$$\sigma_\theta=\sigma_r-ik_1\omega\left(f'-\frac{f}{r}\right)\exp(mi\zeta), \quad \sigma_z=\sigma_r-ik_1\omega\left(f'+\frac{\psi}{r}\right)\exp(mi\zeta)$$

$$\tau_{rz}=0{,}5k_1\omega T\exp(mi\zeta) \tag{1.6}$$

where $\omega = \omega(r) = e_0^{(m-1)/2}$.

From (1.1) and (1.2) we get

$$\sigma_r=H(z)-ik_1\exp(mi\zeta)\int_a^r\omega\left(\frac{m}{2}T+\left(\frac{f}{r}\right)'\right)dr \tag{1.7}$$

From relations (1.1), (1.6), (1.7) we find the unknown function H(z), and for function f we get the fourth order differential equation

$$H(z)=ik_1C_1\exp(mi\zeta)$$

$$(\omega T)''-m\lambda^2\omega\left(mT+2\left(\frac{f}{r}\right)'\right)-2m\lambda^2\left(\omega\left(\frac{\psi}{r}+f'\right)\right)'+\left(\frac{\omega T}{r}\right)'=0 \tag{1.8}$$

where $C_1$ is a constant.

Boundary conditions take the form

$$\tau_{rz}(a,z)=\mu_1\sigma_r(a,z), \quad \tau_{rz}(b,z)=\mu_2\sigma_r(b,z) \tag{1.9}$$

$$u(b,z)=0. \quad u(a,z)=\nu u_1\exp(\nu z-b) \tag{1.10}$$

where $\mu_1$ and $\mu_2$ are coefficients of friction. Moreover, the condition

$$\int_a^b\sigma_z(r,l)rdr=0 \tag{1.11}$$

must be satisfied on end z = *l*.

We introduce dimensionless variables

$$u_0=\frac{u_1}{b}, \quad \nu=\lambda b, \quad \rho=\frac{r}{b}, \quad \rho_0=\frac{a}{b}, \quad \zeta=\frac{z}{b}, \quad \zeta_0=\frac{l}{b}$$

$$u(r,z)=bu^*(\rho,\zeta), \quad w(r,z)=bw^*(\rho,\zeta), \quad \tau_{rz}(r,z)=k_1\tau^*_{rz}(\rho,\zeta) \tag{1.12}$$

$$\sigma_r(r,z)=k_1\sigma^*_r(\rho,\zeta), \quad \sigma_\theta(r,z)=k_1\sigma^*_\theta(\rho,\zeta), \quad \sigma_z(r,z)=k_1\sigma^*_z(\rho,\zeta)$$

$$f(r)=b^2f^*(\rho), \quad R(z)=bR^*(\zeta), \quad C_1=bC_1^*$$

Fourth order differential equation (1.8) can be replaced by a system of four second order differential equations. In dimensionless quantities, it takes the form

$$\frac{df^*}{d\rho}=\frac{\rho\varphi^*-f^*}{2\rho},\quad \frac{d\varphi^*}{d\rho}=\frac{3+4\nu^2\rho^2}{2\rho^2}f^*-\frac{\varphi^*}{2\rho}-2T^*$$

$$\frac{dF^*}{d\rho}=m\nu^2\omega^*\left(mT^*+\frac{\rho\varphi^*-3f^*}{\rho^2}\right) \tag{1.13}$$

$$\frac{dT^*}{d\rho}=\frac{1}{Q^*}\Bigg(8\rho^3F^*\left(\frac{T^{*2}}{4}+\nu^2\frac{3f^{*2}+\rho^2\varphi^{*2}}{4\rho^2}\right)^{\frac{3-m}{2}}+2(1-m)\nu^2\rho(2\nu^2\rho^2+3)f^*\varphi^*T^*-$$

$$-3(5-3m)\nu^2f^{*2}T^*-(3-m)\nu^2\rho^2\varphi^{*2}T^*+4(2m-1)\nu^2\rho^3\varphi^*T^{*2}-$$

$$-2\rho^2T^{*3}+4m\nu^4\rho\varphi^*(3f^{*2}+\rho^2\varphi^{*2})\Bigg)$$

where

$$\varphi^*=\frac{\varphi}{b}=2f^{*\prime}+\frac{f^*}{\rho},\quad T^*=T=\nu^2f^*-\left(\frac{(\rho f^*)'}{\rho}\right)'$$

$$\omega^*=(e_0^*)^{\frac{m-1}{2}}=\omega,\quad e_0^*=e_0=\nu^2\frac{3f^{*2}+\rho^2\varphi^{*2}}{4\rho^2}+\frac{T^{*2}}{4} \tag{1.14}$$

$$F^*=bF=(T^*\omega^*)'-2m\nu^2\varphi^*\omega^*+T^*\omega^*/\rho$$

$$Q^*=b^{-3}Q=2\rho(\nu^2(3f^{*2}+\rho^2\varphi^{*2})+m\rho^2T^{*2})$$

Using relations (1.6), (1.7), (1.12), (1.14), we can find the dimensionless components of stresses

$$\sigma_r^*=\nu(C_1^*+z_1(\rho))\exp(m\nu\zeta),\quad \sigma_\theta^*=\nu\left(C_1^*-\omega^*\frac{\rho\varphi^*-3f^*}{2\rho}+z_1(\rho)\right)\exp(m\nu\zeta)$$

$$\sigma_z^*=\nu(C_1^*-\varphi^*\omega^*+z_1(\rho))\exp(m\nu\zeta),\quad \tau_{rz}=0{,}57\,\omega^*\exp(m\nu\zeta) \tag{1.15}$$

where

$$z_1(\rho)=0{,}5\int_{\rho_0}^{\rho}\omega^*\left(\frac{3f^*-\rho\varphi^*}{\rho^2}-mT^*\right)d\rho$$

$$C_1^*=\frac{0{,}5}{1-\rho_0^2}\int_{\rho_0}^{1}\omega^*\left(3\left(1-\frac{1}{\rho^2}\right)f^*+\left(3+\frac{1}{\rho^2}\right)\rho\varphi^*+m(1-\rho^2)T^*\right)d\rho \tag{1.16}$$

The value of $C_1^*$ in (1.16) is obtained from (1.11).

Boundary conditions and dimensionless quantities take the form

$$T^*(\rho_0)\omega^*(\rho_0)=2\mu_1\nu C_1, \quad T^*(1)\omega^*(1)=2\mu_2\nu(C_1+\varkappa_1(1)), \quad f^*(1)=0, \quad f^{*\prime}(\rho_0)=u_0 \tag{1.17}$$

2. At a small value of parameter $\nu$ we set

$$f^*=\bar{f}, \ \varphi^*=\bar{\varphi}, \ T^*=\nu\bar{T}, \ F^*=\nu^m\bar{F}, \ e_0^*=\nu^2\bar{e}_0, \ Q^*=\nu^2\bar{Q}, \ C_1=\nu^{m-1}\bar{C}_1 \tag{2.1}$$

where

$$\bar{f}=f_0+\nu f_1+\nu^2 f_2+\ldots; \quad \bar{\varphi}=\varphi_0+\nu\varphi_1+\nu^2\varphi_2+\ldots$$

$$\bar{T}=T_0+\nu T_1+\nu^2 T_2+\ldots; \quad \bar{F}=F_0+\nu F_1+\nu^2 F_2+\ldots$$

$$\bar{e}_0=\frac{3\bar{f}^2+\rho^2\bar{\varphi}^2}{4\rho^2}+\frac{\bar{T}^2}{4}=e_{00}+\nu e_{01}+\nu^2 e_{02}+\ldots \tag{2.2}$$

$$\bar{Q}=2\rho(3\bar{f}^2+\rho^2\bar{\varphi}^2+m\rho^2\bar{T}^2)=Q_0+\nu Q_1+\nu^2 Q_2+\ldots$$

$$\bar{C}_1=\frac{0.5}{1-\rho_0^2}\int_{\rho_0}^{1}\bar{\omega}\left(3\left(1-\frac{1}{\rho^2}\right)\bar{f}+\left(3+\frac{1}{\rho^2}\right)\rho\bar{\varphi}+m\nu(1-\rho^2)\bar{T}\right)d\rho=$$

$$=C_{10}+\nu C_{11}+\nu^2 C_{12}+\ldots; \quad \bar{\omega}=\bar{e}_0^{\frac{m-1}{2}}$$

Considering relations (2.2) at $\nu = 0$, (1.13) and (1.17) give the system of equations

$$\frac{df_0}{d\rho}=\frac{\rho\varphi_0-f_0}{2\rho}; \quad \frac{d\varphi_0}{d\rho}=\frac{3f_0-\rho\varphi_0}{2\rho^2}; \quad \frac{dF_0}{d\rho}=0$$

$$\frac{dT_0}{d\rho}=\frac{1}{Q_0}(8\rho^3F_0\omega_0+6(1-m)\rho f_0\varphi_0T_0-3(5-3m)f_0^2T_0-(3-m)\rho^2\varphi_0^2T_0-2\rho^2T_0^3) \tag{2.3}$$

and boundary conditions

$$f_0(1)=0; \quad f_0(\rho_0)=u_0; \quad T_0(\rho_0)\omega_0(\rho_0)=2\mu_1C_{10}$$

$$T_0(1)\omega_0(1)=\mu_2\left(2C_{10}+\int_{\rho_0}^{1}\omega_0\frac{3f_0-\rho\varphi_0}{\rho^2}d\rho\right) \tag{2.4}$$

where

$$e_{00}=\frac{3f_0^2+\rho^2\varphi_0^2}{4\rho^2}+\frac{T_0^2}{4}, \quad Q_0=2\rho(3f_0^2+\rho^2\varphi_0^2+m\rho^2T_0^2)$$

$$C_{10}=\frac{0,5}{1-\rho_0^2}\int_{\rho_0}^{1}\omega_0\left(3\left(1-\frac{1}{\rho^2}\right)f_0+\left(3+\frac{1}{\rho^2}\right)\rho\varphi_0\right)d\rho; \quad \omega_0=e_{00}^{\frac{m-1}{2}} \tag{2.5}$$

Solving the first three equations of (2.3) and satisfying the first two boundary conditions of (2.4), we find

$$f_0 = C_3\left(\frac{1}{\rho} - \rho\right), \quad \varphi_0 = -C_3\left(3 + \frac{1}{\rho^2}\right), \quad F_0 = 2C_4 \tag{2.6}$$

where $C_3 = \rho_0 u_0/(1 - \rho_0^2)$ and $C_4$ is an arbitrary constant.

Substituting (2.6) in the last equation of system (2.3) and making necessary simplifications, we get a nonlinear differential equation for $T_0$

$$\frac{dT_0}{d\rho} = \frac{2C_4\rho\left(C_3^2\left(3 + \frac{1}{\rho^4}\right) + \frac{T_0^2}{4}\right)^{\frac{3-m}{2}} - C_3^2\left(3 + \frac{3-2m}{\rho^4}\right)T_0 - \frac{T_0^3}{4}}{\rho\left(C_3^2\left(3 + \frac{1}{\rho^4}\right) + m\frac{T_0^2}{4}\right)} \tag{2.7}$$

whose integral takes the form

$$C_3^2\left(3 + \frac{1}{\rho^4}\right) + \frac{T_0^2}{4} = \left(\frac{\rho T_0}{C_5 + C_4\rho^2}\right)^{\frac{2}{1-m}} \tag{2.8}$$

where $C_5$ is an arbitrary constant.

Constants $C_4$ and $C_5$ are determined from the last two conditions of (2.4) which, after substitution of $f_0$ and $\varphi_0$, take the form

$$\begin{aligned} C_5 + C_4\rho_0^2 &= -\frac{4C_3\mu_1\rho_0}{1-\rho_0^2}\int_{\rho_0}^{1}\left(3 + \frac{1}{\rho^4}\right)\frac{C_5 + C_4\rho^2}{T_0}\,d\rho \\ C_5 + C_4 &= -\frac{4C_3\mu_2}{1-\rho_0^2}\int_{\rho_0}^{1}\left(3 + \frac{\rho_0^2}{\rho^4}\right)\frac{C_5 + C_4\rho^2}{T_0}\,d\rho \end{aligned} \tag{2.9}$$

At m = 1, we find from (2.8)

$$T_0 = \frac{C_5 + C_4\rho^2}{\rho} \tag{2.10}$$

and conditions (2.9) take the form

$$C_5 + C_4\rho_0^2 = -2C_3\mu_1(3\rho_0^2 + 1)\rho_0, \quad C_5 + C_4 = -8C_3\mu_2 \tag{2.11}$$

At m = 0, we get

$$T_0 = 2C_3\sqrt{3 + \frac{1}{\rho^4}}\,\frac{C_5 + C_4\rho^2}{\sqrt{4\rho^2 - (C_5 + C_4\rho^2)^2}} \tag{2.12}$$

and at m = 0.5

$$T_0=\frac{C_5-C_4\rho^2}{2\sqrt{2}\rho^2}\left[\sqrt{(C_5+C_4\rho^2)^2+\sqrt{(C_5+C_4\rho^2)^4+64C_3^2(1+3\rho^4)}}\right] \qquad (2.13)$$

The problem has been numerically studied at $\mu_1 = 0.3$, $\mu_2 = 0.2$, $a = 10$, $b = 12.5$, $u_1 = 20$, $\nu = 0.025$ ($u_0 = 1.6$, $\rho_0 = 0.8$) for different values of m: m = 0.1, 0.2,..., 0.9. Values of $P^*/\zeta_0$ have been calculated, where $P^* = P/(k_1 b^2)$, P is the force of pressing

$$P=2\pi\int_0^{\zeta_0} R^*\sqrt{1+R^{*2}}\,p^*\,d\zeta\approx\pi\zeta_0\nu^m\left(\rho_0+\nu\left(u_0+\frac{\rho_0 m\zeta_0}{2}\right)\right)T_0(\rho_0)\omega_0(\rho_0) \qquad (2.14)$$

$$\sqrt{1+R^{*2}}\,p^*=-\tau_z^*(\rho_0,\zeta)R^{*\prime}+\tau_{rz}^*(\rho_0,\zeta)$$

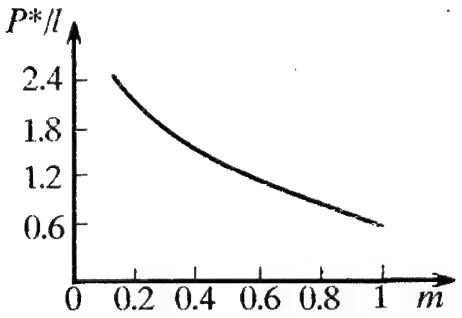

Fig. 2

Fig. 2 shows how $P^*/l$ depends on the quantity m.

*3.* In the case of external introduction (Fig. 3) $R^* = 1 - \nu u_0 \exp(\nu\zeta)$ and the boundary conditions take the form

$$\tau_{rz}(a,z)=\mu_2\sigma_r(a,z),\quad \tau_{rz}(b,z)=\mu_1\sigma_r(b,z) \qquad (3.1)$$

$$u(b,z)=-\nu u_1\exp(\nu z/b),\quad u(a,z)=0 \qquad (3.2)$$

Formulas (1.1)-(1.8), (1.11)-(1.16), (2.1)-(2.3) hold in this case, while the remaining formulas change

$$T^*(\rho_0)\omega^*(\rho_0)=2\mu_2\nu C_1,\quad T^*(1)\omega^*(1)=2\mu_1(C_1^*+\tau_1(1)) \qquad (3.3)$$

$$f^*(1)=-u_0,\quad f^*(\rho_0)=0$$

$$f_0(1)=-u_0,\quad f_0(\rho_0)=0,\quad T_0(\rho_0)\omega_0(\rho_0)=2\mu_2 C_{10}$$

$$T_0(1)\omega_0(1)=2\mu_1\left(C_{10}+\frac{1}{2}\int_{\rho_0}^{1}\omega_0\,\frac{3f_0-2\tau_0}{\rho^2}\,d\rho\right) \qquad (3.4)$$

$$f_0=-C_3\left(\frac{\rho}{\rho_0}-\frac{\rho_0}{\rho}\right),\quad \tau_0=-C_3\left(\frac{3}{\rho_0}-\frac{\rho_0}{\rho^2}\right),\quad F_0=2C_4 \qquad (3.5)$$

$$e_{00}=C_3^2\left(\frac{3}{\rho_0^2}-\frac{\rho_0^2}{\rho^4}\right)+\frac{T_0^2}{4},\quad C_{10}=8\rho^4\left(C_3^2\left(\frac{3}{\rho_0^2}+\frac{\rho_0^2}{\rho^4}\right)+m\frac{T_0^2}{4}\right) \qquad (3.6)$$

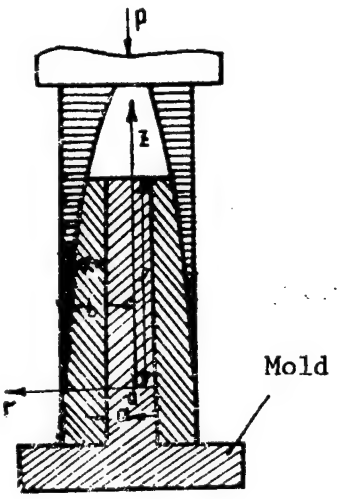


Fig. 3

$$T_0'=\frac{8\rho^3\left(2C_1e_{00}^{\frac{3-m}{2}}-C_3^2\left(\frac{3}{\rho_0^2}+(3-2m)\frac{\rho_0^2}{\rho^4}\right)\frac{T_0}{\rho}-\frac{T_0^3}{4\rho}\right)}{Q_0} \tag{3.7}$$

$$C_3^2\left(\frac{3}{\rho_0^2}+\frac{\rho_0^2}{\rho^4}\right)+\frac{T_0^2}{4}=\left(\frac{\rho T_0}{C_5+C_4\rho^2}\right)^{\frac{2}{1-m}} \tag{3.8}$$

$$C_{10}=-\frac{2C_3}{1-\rho_0^2}\int_{\rho_0}^{1}\left(\frac{\rho_0}{\rho^3}+3\frac{\rho}{\rho_0}\right)\omega_0 d\rho \tag{3.9}$$

$$C_5+C_4\rho_0^2=-\frac{4\mu_2C_3}{1-\rho_0^2}\int_{\rho_0}^{1}\left(\frac{\rho_0^2}{\rho^4}+3\right)\frac{C_5+C_4\rho^2}{T_0}\,d\rho$$

$$C_5+C_4=-\frac{4\mu_1C_3}{1-\rho_0^2}\int_{\rho_0}^{1}\left(\frac{3}{\rho_0}+\frac{\rho_0^3}{\rho^4}\right)\frac{C_5+C_4\rho^2}{T_0}\,d\rho \tag{3.10}$$

If m = 1, then

$$T_0=\frac{C_5+C_4\rho^2}{\rho} \tag{3.11}$$

$$C_5+C_4\rho_0^2=-8\mu_2C_3,\quad C_5+C_4=-2\mu_1C_3(3+\rho_0^2)/\rho_0 \tag{3.12}$$

REFERENCES

1. Zadoyan, M. A., "Introduction of Rigid Cylindrical Body Into Ideally Plastic Tube," MEKHANIKA TVERDOGO TELA, No 5, 1985, pp 98-108.

2. Akopyan, A. G., Zadoyan, M. A., "Introduction of Rigid Cylindrical Body Into Plastically Anisotropic Tube," IZVESTIYA AKADEMII NAUK ARMYANSKOY SSR: SERIYA MEKHANIKA, Vol 39, No 5, 1986, pp 27-36.

3. Akopyan, A. G., "Screwing Rigid Cylindrical Body Into Plastically Anisotropic Tube," IZVESTIYA AKADEMII NAUK ARMYANSKOY SSR: SERIYA MEKHANIKA, Vol 39, No 6, 1986, pp 25-38.

# ELECTRICAL TRANSIENT PROCESSES IN THE VAPOR-GAS SHELL UNDER CONDITIONS OF ELECTROLYTIC ANODIC HEATING WITH RECTANGULAR VOLTAGE PULSES

907F0366A Kishinev ELEKTRONNAYA OBRABOTKA MATERIALOV in Russian No 2, 1990 pp 36-38

[Article by S. I. Galanin, V. I. Ganchar, and E. G. Dmitriyev, Institute of Applied Physics, Moldavian SSR Academy of Sciences]

[Text] Anodic electrolytic heating (AEH) is accompanied by film boiling of the electrolyte solution on the surface of the anode. The two-phase system which results is electrically conductive, and the existence of a vapor film (shell) around the anode results from the joulian heat release of the current flowing through it. One of the methods of obtaining information about the nature of the current carriers in the gaseous phase is analysis of the dependence of the electrical conductivity of the vapor-gas shell on the applied voltage. However, such dependence cannot be obtained directly from the volt-ampere characteristic of the stationary process of AEH, for in stationary conditions the change in electrical resistance of the shell under change in the voltage results primarily from change in the thickness of the shell [1]. The required dependence of the shell conductivity on the applied voltage may be obtained by pulsed measurement methods. In the most simple experimental layout for a pulse technique, it is sufficient to measure the time constant of decay of the discharge current of a capacitor of given capacitance through the shell. Such a simple method is only useful when the shell represents a purely active resistance. In reality, when the electric field is turned on in pulses, the phase boundaries of the regions near the electrodes are charged and dual electric layers are created on them, which may be approximated as capacitors having a certain overall capacitance $C_п$. In order to clarify the influence of this capacitance on the measurements of electrical conductance of the shell, it is necessary to know its magnitude. This is the task of the present work.

In order to measure the magnitude of the overall surface capacitance $C_п$, rectangular voltage pulses were used. A steel anode was heated in a stationary AEH process up to $T \gtrsim 800°C$, and then the voltage was switched off. A single rectangular voltage pulse was applied to the thus-prepared current-free shell in a time much shorter than its persistence time. The results of the action of this pulse on the electrolytic cell with and without an anode vapor shell present in it were qualitatively different (see Fig. 1): the electrolytic cells does not distort the original shape of the imposed pulse; a distortion is only observed when the current-free anode shell is present in

the system. This experimental fact suggests that the presence of the current-free anode shell in the electrolytic cell brings about an additional capacitance in the system, sufficient to distort significantly the shape of the imposed pulse.

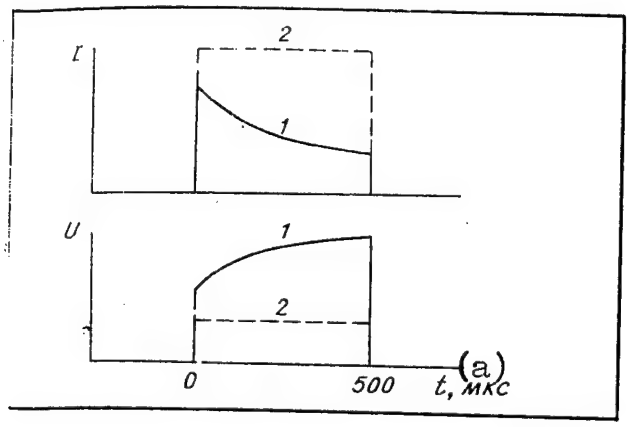


Fig. 1. Comparison of current and voltage oscillograms obtained with a rectangular voltage pulse acting on an electrolytic cell in the presence (1) and absence (2) of a current-free vapor shell in it.
Key: a. μs.

It is easy to support this conclusion with calculation. For this, we represent the electrolytic cell with current-free anodic shell present in it as an equivalent substitution circuit (Fig. 2). The current and voltage measured by the oscillograph may be obtained from the system of equations:

$$\begin{cases} U_0 = I_0(R_\text{п} + R_\text{э} + R_\text{об}) + I_R R_\text{п}, \\ \dfrac{1}{C}\int_0^t I_C dt = I_R \cdot R_\text{п} \\ I_0 = I_R + I_C, \; I_R(0) = 0, \end{cases} \tag{1}$$

where $U_0$ is the potential of the source of rectangular pulses; $I_0$ is the current flowing through the electrolytic cell, $I_R$ and $I_C$ are the currents flowing through the active resistance of the phase interface surfaces $R_\text{П}$ and the overall surface capacitance $C_\text{П}$, respectively; $R_\text{и}$, $R_\text{э}$, and $R_\text{об}$ are the internal resistance of the source and the active resistances of the electrolyte and shell, respectively. From (1), we obtain for the sought quantities U(t) and $I_0(t)$:

$$U(t) = U_0 \frac{R_1}{R_2}\left\{1 + \frac{R_\text{п} R_\text{и}}{R_1 R_3}\left[1 - \exp\left(-\frac{R_2}{R_2}\frac{t}{C_\text{п} R_\text{п}}\right)\right]\right\}, \tag{2}$$

$$I_0(t) = \frac{U_0}{R_2}\left\{1 - \frac{R_\text{п}}{R_3}\left[1 - \exp\left(-\frac{R_3}{R_2}\frac{t}{C_\text{п} R_\text{п}}\right)\right]\right\}, \tag{3}$$

where $R_1 = R_э + R_{об}$, $R_2 = R_э + R_{об} + R_и$, $R_3 = R_э + R_{об} + R_и + R_п$.

Calculation by (2) and (3) yields time functions U(t) and $I_0(t)$, similar to the experimental. The observed distortion in shape of the imposed pulse is achieved when $C_п \gtrsim 2000$ $\mu$F for values of $R_1$, $R_2$, and $R_3$ on the order of 0.1-1 ohms and duration of the imposed pulse $\tau$ = 500 $\mu$s.

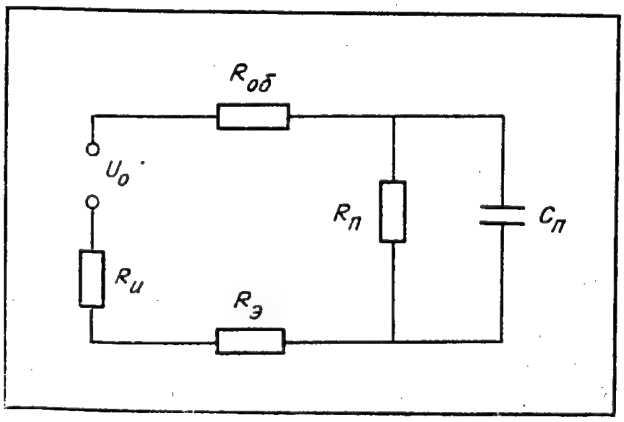


Fig. 2. Equivalent electrical substitution circuit of an electrolytic cell with current-free vapor shell present in it.

The surface capacitance of the phase interface boundary can also be evaluated from other considerations. As an example, consider an electrolyte-vapor interface surface. Under the action of the imposed voltage, the phase boundary is charged until the electric field of the surplus charge accumulating on the surface cancels out the external field. The characteristic dimension of the charge separation will be the Debye screening radius, which is connected to the equilibrium charge density within the electrolyte n by the familiar relation:

$$r_D = (\varepsilon T / 4\pi e^2 n)^{1/2}. \qquad (4)$$

Here, T is the temperature of the electrolyte near the surface, expressed in energy units; e is the charge of the electron; $\varepsilon$ is the dielectric permittivity of the electrolyte near the phase boundary. The surface layer of electrolyte, $r_D$ thick, may be approximated as a flat capacitor, the capacitance of which is:

$$C_п = \varepsilon\varepsilon_0 / r_D, \qquad (5)$$

where $\varepsilon_0 = 8.85 \cdot 10^{-12}$ F/m is the dielectric constant. As a result, we find that $C_п \sim \sqrt{n}$, and as the electrolyte concentration varies from 13 to 38 percent the specific surface conductivity of the electrolyte-vapor phase boundary changes from 0.82 to 1.5 F/m$^2$. In the conditions under which the measurements were taken, the anode surface was $2.7 \cdot 10^{-3}$ m$^2$; thus, the total capacitance of the phase surface should change from 2200 to 3900 $\mu$F as the electrolyte

concentration varies in the indicated range. Such dependence of the surface capacitance on the electrolyte concentration is experimentally confirmed: as the electrolyte concentration rises, the shape of the imposed voltage pulses is more heavily distorted (Fig. 3).

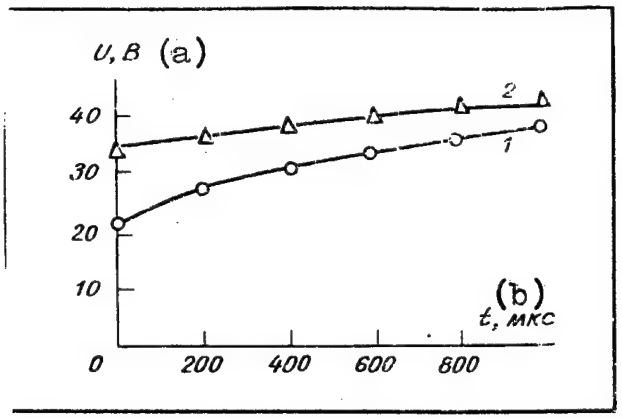


Fig. 3. Oscillograms of voltage at various concentrations of electrolyte $NH_4NO_3$: 1 - 32 percent, 2 - 13 percent. Solid lines - calculation, points - measurement results.
Key:
a. V b. μs.

As for the nature of the influence of the surface capacitance of the phase boundaries on the pulse measurement results, it may be variable. For example, when low-voltage pulses are applied to the current-free anode shell and the potential $U_0$ is less than a certain critical value $U_{кр}$, there are no conduction currents through the vapor shell [2], and the surface capacitance $C_п$ in the equivalent substitution circuit is connected in series with the proper capacitance of the shell $C_{об}$. Since $C_{об} \ll C_п$, the overall capacitance of the system is $C \approx C_{об}$. Thus, the influence of the surface capacitance is eliminated, making it possible to measure the proper capacitance of the anode shell. Such measurements were performed in [3]; according to the data of this work, $C_{об}$= (150-300) pF. A different situation occurs when measuring the conductance of the anode shell: when a capacitor charged to potential $U_0 > U_{кр}$ is connected to the shell, a discharge current flows through it; the capacitance of the phase interface surface is added to the capacitance being discharged. The capacitance of the phase interface surface is on the order of thousands of microfarads, while the electrolyte-vapor phase surface is able to discharge in a time on the order of hundreds of microseconds. Consequently, in order to eliminate the influence of the capacitance of the phase boundary on the measurements, the discharging capacitance must be chosen in the range of values much larger than the capacitance of the phase boundary, and the current decay curve must be registered in the millisecond time range in a period longer than the charge time of the phase interface surface.

## Bibliography

1. Ganchar, V. I., Dmitriyev, E. G., "The Volt-Temperature and Volt-Ampere Characteristics of the Electrolytic Anode Heating Process," ELEKTRONNAYA OBRABOTKA MATERIALOV, No 2, 1989, pp. 23-25.

2. Belkin, P. N., Ganchar, V. I., Petrov, Yu. N., "An Investigation of the Conduction of the Vapor Film During Anode Electrolytic Heating," DAN SSSR, Vol 291, No 5, 1986, pp. 1116-1119.

3. Duradzhi, V. N., Bryantsev, I. V., "Several Parameters of the Electric Circuit of the Anode Process During Heating of Metals in Electrolytic Plasma," ELEKTRONNAYA OBRABOTKA MATERIALOV, No 1, 1981, pp. 40-43.

# INVESTIGATION OF AN UNDERWATER ELECTRIC EXPLOSION INITIATED BY FERROMAGNETIC PARTICLES. I. PHYSICAL MODELING

907F0366B Kishinev ELEKTRONNAYA OBRABOTKA MATERIALOV in Russian No 2, 1990 pp 44-48

[Article by L. Z. Boguslavskiy, L. M. Bondarets, V. V. Kucherenko, and V. V. Shamko, Electrohydraulic Design Development Office, Ukrainian SSR Academy of Sciences]

[Text] The results of experimental studies of an electrical explosion in ferromagnetic suspensions [1, 2] show that, depending on the conduction and concentration of the solid phase, both the conditions of formation of the channel and the discharge regime vary. This should result in change in the gas dynamic characteristics of the underwater electrical explosion (UEE) and, accordingly, the effectiveness of transformation of electrical energy into mechanical [3, 4]. Therefore, the present work is devoted to developing the methods of calculation of the energy and gas dynamic characteristics of an electric explosion in a liquid containing ferromagnetic inclusions.

In the first part of the work, the methods of physical modeling are used to investigate the electrical, energy, and kinematic characteristics of the UEE with initiation by ferromagnetic particles, localized in lengthwise bridges.

The experiments were carried out in a tank (0.9 x 0.9 x 0.6 $m^3$) with portholes of organic glass, filled with distilled water of electric conductance $\sigma_0 \approx 2.5 \cdot 10^{-3}$ $\Omega^{-1} \times m^{-1}$ (the layout is similar to that of [5]). In order to reduce the cumulative effect of the electric explosion cavity (EEC), the negative electrode had a rectangular opening of 0.03 x 0.23 x 0.1 $m^3$ (the external appearance of the electrode system with ferromagnetic bridge is shown in Fig. 1). The distance between electrodes in all cases was $l$ = 40 mm, and the discharge occurred at depth of 0.3 m.

The bridges were created from ferromagnetic powder SF-35 with initial electric conductivity $\sigma_0 = 10^{-2}$ $\Omega^{-1} \cdot m^{-1}$ as follows. In a separate vessel, a 10 percent suspension of powder SF-35 was prepared from distilled water, and a capillary was used to supply this to the interelectrode gap (IEG) with a lengthwise magnetic field, created by a special coil [1]. When the suspension enters the region of the field, the solid particles line up along the field lines and form a bridge spanning the entire IEG (see Fig. 1).

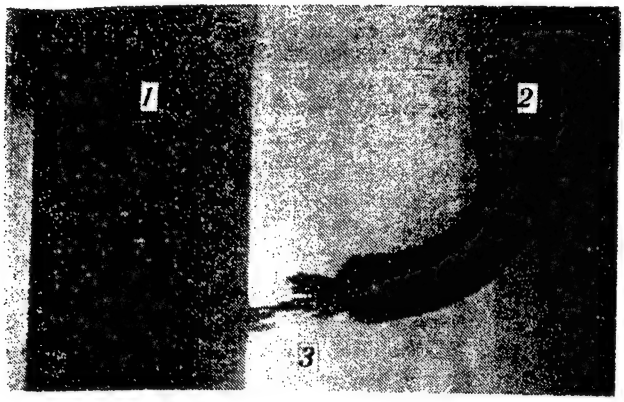


Fig. 1. External appearance of electrode system and ferromagnetic bridge: 1 - negative electrode; 2 - positive electrode; 3 - ferromagnetic bridge.

The electrotechnical parameters (charge voltage of the capacitor bank $U_0$, its capacitance C, the inductance of the discharge circuit L) are presented in Table 1. For each particular set of parameters $U_0$, C, L, at least 13-15 discharges were performed, and the obtained results were averaged.

Table 1. Electrotechnical parameters of the discharge circuit

| Номер разряда (a) | $U_0$, $10^1$ В (b) | C, $10^{-6}$ Ф (c) | $W_0$, Дж (d) |
|---|---|---|---|
| 1 | 20 | 6 | 1200 |
| 2 | 30 | 6 | 2700 |
| 3 | 20 | 12 | 2400 |

Key: a. Number of discharge
b. V c. F d. J

NOTE: L, $10^{-6}$ = 3.5 H.

The studies were done by the method simultaneous registration of electric and space-time characteristics of the discharge channel and the EEC. The current was registered by a low-resistance coaxial shunt, the voltage drop across the discharge gap by a capacitive divider, the signals from which were sent to the S8-17 oscillograph. The inductive component of the voltage drop was compensated. The discharge channel was photographed by the high speed camera VFU-1, acting as a photoregister (mirror rotational speed 30,000 rpm), the cavity was photographed by the SFR-2M with an adapter reducing the mirror turning speed by two orders of magnitude. Highlighting during investigation of the channel stage was provided by the pulse lamp IFK-2000, and after the discharge the constant light source KG-110 was used.

The current and voltage oscillograms (similar to those presented in [1] were used to determine: in the channel formation stage, the breakdown delay time $t_з$, the decrease in magnitude of the initial potential $\Delta U_0$, the energy losses $\Delta W$ (averaged values of these are given in Table 2 for the different discharge regimes), and in the active stage the energy generated in the channel W(t), the time for its generation $\tau$, and the electric power N(t). Deviations of the investigated quantities from the mean values usually did not exceed 30 percent for $t_з$, 50 percent for $\Delta U_0$, 10 percent for $\tau$, and 15 percent for $\Delta W/W_0$.

Table 2. Averaged time and energy characteristics of discharges 1-3

| Номер разряда (a) | $\overline{t_з}$, мкс (b) | $\overline{\Delta U_0}$, кВ (c) | $\overline{\Delta W}/W_0$, % | $\overline{\eta}$ | $\overline{l_э}$, мм |
|---|---|---|---|---|---|
| 1 | 39 | 1.5 | 14 | 0.73—0.87 | 90—116 |
| 2 | 14 | 1,9 | 12 | 0,55—0,72 | 89—133 |
| 3 | 36 | 1,5 | 14 | 0.6—0.8 | 80—120 |

Key:

a. Number of discharge

b. $\mu$s

c. kV

A characteristic of the formation of the channel when the discharge is initiated by powder SF-35 is the fact that, within 20-30 $\mu$s after voltage is applied to the IEG, several luminous regions of size 1-2 mm are created at its center, the number of which increases in the lengthwise direction over the course of time (Fig. 2a, b). Occasionally, two luminous chains appear, spanning the entire gap at a certain instant.

The mechanism of formation of the discharge channel (breakdown stage) when the discharge is initiated by conductive ferromagnetic inclusions has been discussed in [1, 2, 6] and is explained by the redistribution of the electric field in the gap as a result of the presence of the bridge, resulting in concentration of current and joulian heat release in individual regions on the surface of the inhomogeneity. The latter, in the opinion of [1, 2, 6], may result in initiation of a discharge in these zones. It may be that a similar breakdown mechanism occurs in a suspension based on the powder SF-35, since its electric conduction is greater than that of water. However, other mechanisms may be at play (breakdown along the surface of the bridge, breakdown of gas bubbles ever present in the liquid, etc.).

It is difficult to distinguish in time and space the stages of formation of the discharge channel (prior to breakdown) and the channel proper, as is obvious from Fig. 2a. Toward this end, the discharge channel was photographed without lighting (see Fig. 2b) and the appearance of an intense diffuse light around the channel in the second frame was coordinated (on the analogy of a discharge without initiation) with the start of a sharp rise in current on the oscillograms. Thus, the electric and kinematic characteristics of the discharge when initiated by ferromagnetic bridge were synchronized.

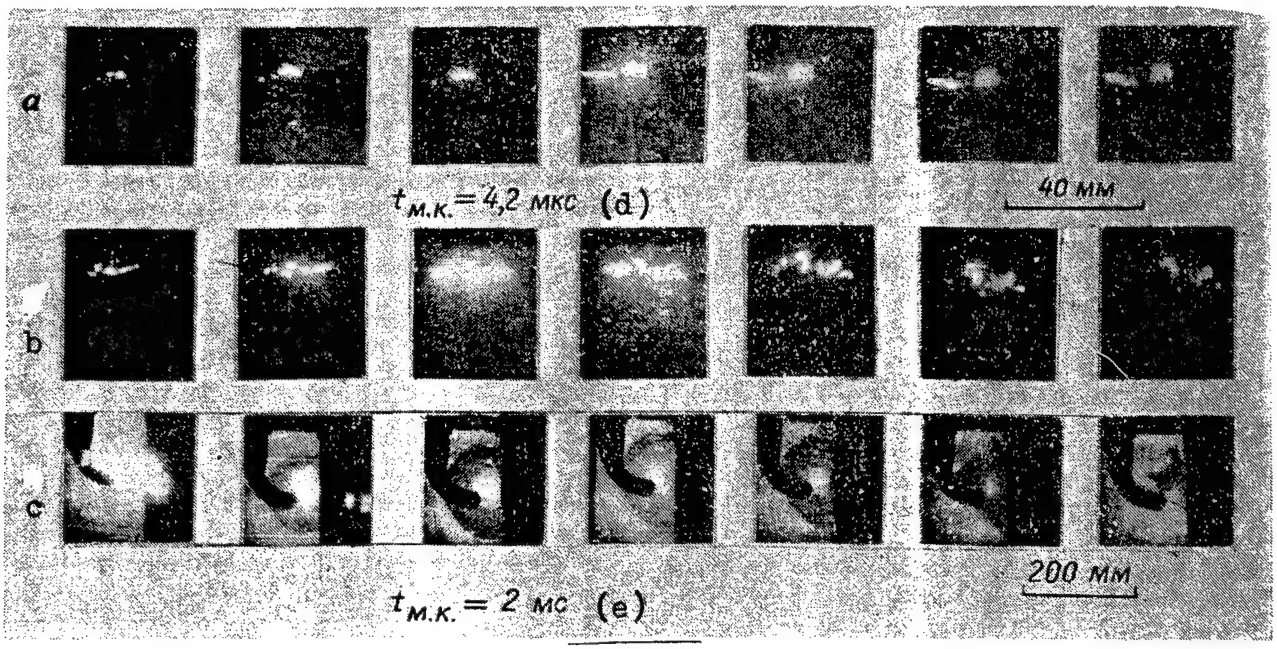


Fig. 2. Motion picture records of the channel and cavity for the first discharge: a, b - discharge channel with UEE initiated by powder SF-35; c - cavity with UEE initiated by copper wire, diameter 0.1 mm.
Key: d. μs e. ms

The resulting discharge channel is not homogeneous either along the lengthwise or radial coordinate (its glow is not uniform), making it hard to determine its kinematic characteristics. Figure 3 shows the functions of the radius of the channel a(t) and the speed of its expansion $\dot{a}(t)$ for the first discharge. The time is counted off from the instant of appearance of glow in the IEG (the stage prior to breakdown is also partly included). These curves are basically qualitative in nature, due to the difficulties of exact determination of the radius of the channel (in the present case, it is determined as the radius of the brightest portion of the channel for a particular cross section that is sufficiently visible in the motion picture records, see Fig. 2a). As is evident from Fig. 3, the parameters of the channel at the instant of closing of the plasma branch of the IEG ($t \approx 30$ μs), i.e., the initial conditions for the channel stage, amount to $a_0 \approx 1$ mm, $\dot{a}_0 \approx 10$ m/s.

Comparison of the experimental curves of the power N(t), obtained in the present work for electric explosion initiated by SF-35 powder (Fig. 4, curve 2) and initiated by microconductor or high-voltage liquid breakdown [3], revealed a qualitative analogy. Previously [3], an analogy was found for the electric and kinematic characteristics of UEE in terms of the parameter:

$$\eta = \left(\frac{\pi A I^2}{U_0 \sqrt{LC}}\right)^{1/3},$$

characterizing the discharge regime and representing the portion of energy released during the first half-period of the current. Here, A is the spark constant, which for an electric explosion initiated by microconductor is $A = 0.25 \cdot 10^5$ $V^2 \cdot s/m^2$.

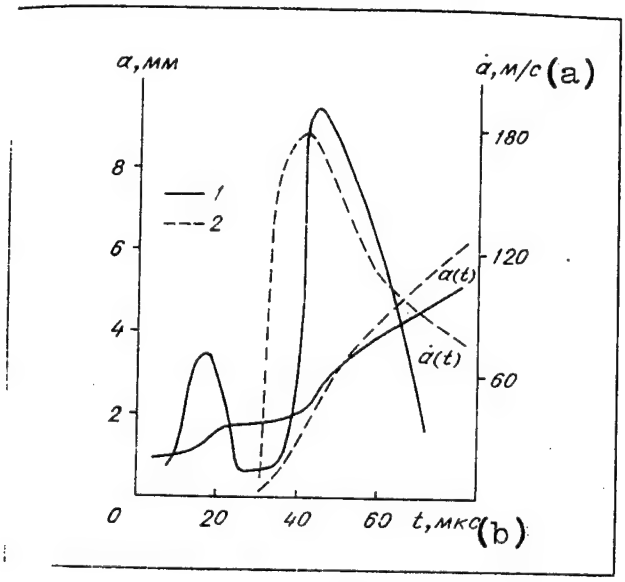


Fig. 3. Time curves of radius of channel a(t) and speed of its expansion ȧ(t) for the first discharge: 1 - experiment, 2 - calculation.
Key: a. m/s b. μs

In the present work, the parameter $\eta$ was determined experimentally as the ratio between the energy $W_1$ released during the first half-period of the current and the stored energy $W_0 = CU_0^2/2$. It turned out that, for unchanged initial electrotechnical parameters of the channel and physico-mechanical properties of the working medium, the parameter changes from one discharge to another (for an UEE initiated by microconductor, the regime is uniquely characterized). The range of change in $\eta$ for discharges 1-3 is shown in Table 2. While for conducting powders [1, 2, 6] this was due to change in concentration of the solid phase in the ferromagnetic suspension and, thus, the initial diameter of the bridge, for the nonconducting powder SF-35 this may be explained by an increase in length of the channel as compared to the length of the IEG (see the above expression for $\eta$). Values of the equivalent channel lengths $l_э$, corresponding to the UEE initiated by microconductor and calculated for different discharge regimes, are presented in Table 2. The above-given results of experimental investigations of the energy characteristics of an electric explosion initiated by SF-35 powder show that they can be determined in accordance with the technique [4] developed for an ordinary underwater spark discharge. However, in calculating the parameter $\eta$, instead of the length of the gap l it is necessary to use $2l \leq l_э \leq 3l$.

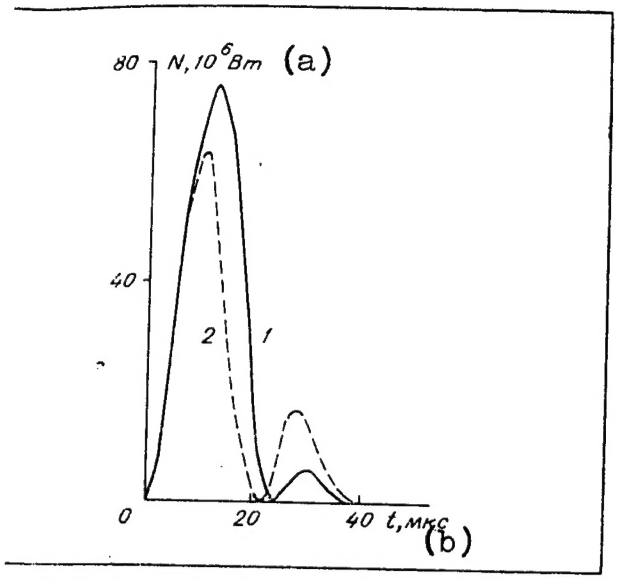


Fig. 4. Power curves for the first discharge: 1 - experiment, 2 - calculation by [4].
Key: a. W b. μs

We investigated the influence of the opening in the negative electrode on the kinematics of the cavity. Since a poor quality of photograph of the EEC is obtained when the UEE is initiated by powder SF-35, Fig. 2c presents photographs for the first discharge initiated by copper conductor of diameter 0.1 mm. During the first pulsation, the cavity is dome shaped, and becomes slightly deformed in the closure stage. It has been established that the shape of the cavity, its maximum volume, and the period of the first pulsation are almost unaffected by the opening, which basically influences the speed of movement of the EEC boundaries (the cavity collapses more intensely if the opening is missing, see Fig. 5a, b) and the number of compression pulses generated by the cavity. Thus, when an opening is present, the EEC produces a single compression wave, and when it is absent (closed by a metal plate), it produces two waves. Analysis of the kinematic characteristics of the EEC (height of the dome $d_{\perp}(t)$, its speed $\dot{d}_{\perp}(t)$ in the perpendicular direction (a) and the radius of the cavity $a_{=}(t)$, the speed $\dot{a}_{\parallel}(t)$ in the direction parallel to the negative electrode, Fig. 5) reveals that the functions more sensitive to presence of an opening are $d_{\perp}(t)$, $\dot{d}_{\perp}(t)$. The kinematic characteristics of the EEC formed during UEE initiated by powder SF-35 for the third discharge are shown in Fig. 5c.

In the concluding stages of the closure (see Fig. 2c), the cavity moves in the direction of the free surface and collapses to form a cumulation stream of liquid, 4 cm above the point of contact between the channel and the plate covering the opening. At the point of impact of the stream on the plate, a conical funnel is formed with radius of depression at the contact point 1-2 mm. Because the regions of influence of the channel and the cavity (stream) are at a distance from each other, it was possible to separate their mechanical action on the plate. It was found that the bending of the plate (using copper and steel strips, $\delta$ = 0.25-1 mm thick) at the point of action of the shaped stream of liquid was several millimeters larger than at the point

of contact of the channel. Thus, for a copper plate with $\delta$ = 0.25 mm, the bending was respectively 10 and 7 mm. This result is consistent with the data of [7, 8].

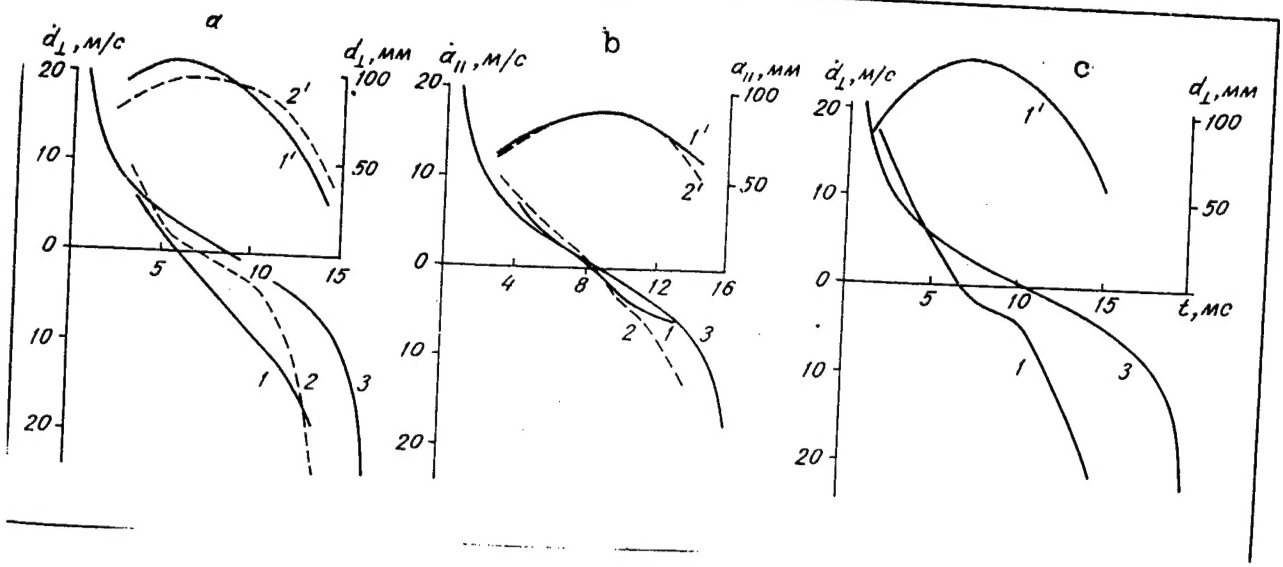


Fig. 5. Kinematic characteristics of cavities: a, b - initiated by copper conductor, 0.1 mm diameter, first discharge; c - initiated by powder SF-35, third discharge; 1, 2 - experiment (primed numbers - radius), 3 - calculation; --- electrode without opening.

Thus, the initiation of a discharge by nonconducting ferromagnetic particles satisfactorily stabilizes its energy, kinematic, and time characteristics.

## Bibliography


1. Demina, V. M., Lyubimov, A. D., Satanovskiy, V. V., "Experimental Studies of the Breakdown of a Ferromagnetic Suspension in an External Magnetic Field," ELEKTRONNAYA OBRABOTKA MATERIALOV, No 4, 1985, pp. 52-56.

2. Nazarova, L. L., Malikov, P. D., Reztsov, V. F., "On Transient Processes in Electric Discharge in Liquid Containing Ferromagnetic Inclusions in an External Lengthwise Magnetic Field," "Fizicheskiye osnovy elektricheskogo vzryva: Sb. nauch. tr." [Physical Foundations of an Electric Explosion: Collection of Scientific Papers], Kiev, 1983, pp. 60-64.

3. Krivitskiy, Ye. V., Shamko, V. V., "Perekhodnyye protsessy pri vysokovoltnom razryade v vode" [Transient Processes in High-Voltage Discharge in Water], Kiev, 1979.

4. Kucherenko, V. V., "Nestatsionarnyye gazodinamicheskiye techeniya pri podvodnom elektrovzryve" [Nonstationary Gas Dynamic Currents in an

Underwater Electric Explosion], Author's Abstract of Dissertation for Candidate of Technical Sciences, Kiev, 1988.

5. Shamko, V. V., Vovchenko, A. I., "Influence of Boundary Surfaces on Development of the Vapor-Gas Cavity in an Underwater Spark Discharge," "Gidromekhanika: Sb. nauchn. tr." [Hydromechanics: Collection of Scientific Papers], Issue 34, Kiev, 1976, pp. 52-60.

6. Malikov, P. D., Nazarova, L. L., Reztsov, V. F., "A Qualitative Model of Initiation of an Electric Discharge in a Conductive Liquid by Inhomogeneities," ZHTF, Vol 55, No 3, 1985, pp. 616-618.

7. Khasiguti Kiyekhito, Yamatoto Takekhisa, "Movement of a Gas Bubble and Impact Force During Discharge of a Capacitor in Liquid," KIKAY TO KOGU, Vol 13, No 11, 1969, pp. 146-154.

8. Chachin, V. N., "Elektrogidravlicheskaya obrabotka mashinostroyitelnykh materialov" [Electrohydraulic Machining of Materials], Minsk, 1978.



- END -

Foreign Broadcast Information Service (FBIS) and Joint Publications Research Service (JPRS) publications contain political, military, economic, environmental, and sociological news, commentary, and other information, as well as scientific and technical data and reports. All information has been obtained from foreign radio and television broadcasts, news agency transmissions, newspapers, books, and periodicals. Items generally are processed from the first or best available sources. It should not be inferred that they have been disseminated only in the medium, in the language, or to the area indicated. Items from foreign language sources are translated; those from English-language sources are transcribed. Except for excluding certain diacritics, FBIS renders personal names and place-names in accordance with the romanization systems approved for U.S. Government publications by the U.S. Board of Geographic Names.

Headlines, editorial reports, and material enclosed in brackets [ ] are supplied by FBIS/JPRS. Processing indicators such as [Text] or [Excerpts] in the first line of each item indicate how the information was processed from the original. Unfamiliar names rendered phonetically are enclosed in parentheses. Words or names preceded by a question mark and enclosed in parentheses were not clear from the original source but have been supplied as appropriate to the context. Other unattributed parenthetical notes within the body of an item originate with the source. Times within items are as given by the source. Passages in boldface or italics are as published.

## SUBSCRIPTION/PROCUREMENT INFORMATION

The FBIS DAILY REPORT contains current news and information and is published Monday through Friday in eight volumes: China, East Europe, Soviet Union, East Asia, Near East & South Asia, Sub-Saharan Africa, Latin America, and West Europe. Supplements to the DAILY REPORTs may also be available periodically and will be distributed to regular DAILY REPORT subscribers. JPRS publications, which include approximately 50 regional, worldwide, and topical reports, generally contain less time-sensitive information and are published periodically.

Current DAILY REPORTs and JPRS publications are listed in *Government Reports Announcements* issued semimonthly by the National Technical Information Service (NTIS), 5285 Port Royal Road, Springfield, Virginia 22161 and the *Monthly Catalog of U.S. Government Publications* issued by the Superintendent of Documents, U.S. Government Printing Office, Washington, D.C. 20402.

The public may subscribe to either hardcover or microfiche versions of the DAILY REPORTs and JPRS publications through NTIS at the above address or by calling (703) 487-4630. Subscription rates will be provided by NTIS upon request. Subscriptions are available outside the United States from NTIS or appointed foreign dealers. New subscribers should expect a 30-day delay in receipt of the first issue.

U.S. Government offices may obtain subscriptions to the DAILY REPORTs or JPRS publications (hardcover or microfiche) at no charge through their sponsoring organizations. For additional information or assistance, call FBIS, (202) 338-6735,or write to P.O. Box 2604, Washington, D.C. 20013. Department of Defense consumers are required to submit requests through appropriate command validation channels to DIA, RTS-2C, Washington, D.C. 20301. (Telephone: (202) 373-3771, Autovon: 243-3771.)

Back issues or single copies of the DAILY REPORTs and JPRS publications are not available. Both the DAILY REPORTs and the JPRS publications are on file for public reference at the Library of Congress and at many Federal Depository Libraries. Reference copies may also be seen at many public and university libraries throughout the United States.